Published in final edited form as:

J Cell Physiol. 2017 May ; 232(5): 1053–1068. doi:10.1002/jcp.25508.

Functional Effects of Cigarette Smoke-Induced Changes in Airway Smooth Muscle Mitochondrial Morphology

Bharathi Aravamudan[1], **Michael Thompson**[1], **Gary C. Sieck**[1,2], **Robert Vassallo**[3], **Christina M. Pabelick**[1,2], and **Y.S. Prakash**[1,2]

[1]Department of Anesthesiology, Mayo Clinic, Rochester, MN 55905 USA

[2]Department of Physiology and Biomedical Engineering, Mayo Clinic, Rochester, MN 55905 USA

[3]Department of Medicine, Mayo Clinic, Rochester, MN 55905 USA

Abstract

Long-term exposure to cigarette smoke (CS) triggers airway hyperreactivity and remodeling, effects that involve airway smooth muscle (ASM). We previously showed that CS destabilizes the networked morphology of mitochondria in human ASM by regulating the expression of mitochondrial fission and fusion proteins via multiple signaling mechanisms. Emerging data link regulation of mitochondrial morphology to cellular structure and function. We hypothesized that CS-induced changes in ASM mitochondrial morphology detrimentally affect mitochondrial function, leading to CS effects on contractility and remodeling. Here, ASM cells were exposed to 1% cigarette smoke extract (CSE) for 48 hours to alter mitochondrial fission/fusion, or by inhibiting the fission protein Drp1 or the fusion protein Mfn2. Mitochondrial function was assessed via changes in bioenergetics or altered rates of proliferation and apoptosis. Our results indicate that both exposure to CS and inhibition of mitochondrial fission/ fusion proteins affect mitochondrial function (i.e., energy metabolism, proliferation and apoptosis) in ASM cells. *In vivo*, the airways in mice chronically exposed to CS are thickened and fibrotic, and the expression of proteins involved in mitochondrial function is dramatically altered in the ASM of these mice. We conclude that CS-induced changes in mitochondrial morphology (fission/ fusion balance) correlate with mitochondrial function, and thus may control ASM proliferation, which plays a central role in airway health.

Keywords

Environmental tobacco smoke; lung; Drp1; Mfn2; metabolism; proliferation; apoptosis; autophagy; remodeling

Address for Correspondence: Y.S. Prakash, MD, Ph.D., Professor of Anesthesiology and Physiology, Chair, Department of Physiology and Biomedical Engineering, 4-184 W Joseph SMH, Mayo Clinic, Rochester MN 55905, (507) 255 7481, (507) 255 7300 (fax), prakash.ys@mayo.edu.

The authors have no conflict of interest to declare.

Introduction

Chronic exposure to cigarette smoke (CS) is known to exacerbate airway diseases such as asthma by contributing to airway hyperresponsiveness and structural changes. Changes in ASM cell proliferation could be a potential mechanism via which CS effects are exerted on the airway (1–7). However, the signaling pathways that mediate CS effects on ASM are still under investigation.

There is now increasing recognition that beyond being vital for energy production and cellular metabolism, mitochondria are key players in reactive oxygen species (ROS) production, calcium buffering and cell fate determination. In this regard, there is also increasing evidence that the dynamic morphology of mitochondrial networks is important. During homeostasis, long, contiguous tracks of fused mitochondria and branching networks predominate (driven by regulatory proteins such as the Mitofusins (Mfn)), while upon exposure to stress (inflammation, environmental factors), mitochondria undergo fission, their networks are unraveled and a fragmented morphology becomes more prominent (regulated by proteins such as Drp1) (8–12). In addition to defining mitochondrial morphology cycling of the fission and fusion events also bears functional importance influencing mitochondrial mixing, integrity of the mitochondrial DNA, cellular adaptability to stress, mitochondrial respiration, and cell fate determination (10).

Considerable evidence has come to light suggesting that mitochondrial morphology (i.e., fission/ fusion balance) is linked to the mitochondrion's primary function, namely energy metabolism (13,14). Since mitochondrial fission-fusion balance is highly sensitive to environmental changes it stands to reason that changes in mitochondrial morphology translate to alterations in mitochondrial function, and in mitochondria-dependent cellular events. For example, while the bioenergetic function of mitochondria has been reported to influence cell proliferation (15–18), mitochondrial fission and fusion have also been shown to influence proliferation (19–23).

The relevance of mitochondrial fission and fusion to ASM structure and function particularly in the context of airway diseases is emerging (24–27). It is now known that CS induces disruption of ASM mitochondrial morphology by regulating expression of proteins responsible for mitochondrial fission and fusion (28,29). However, the downstream effects of altered ASM mitochondrial fission and fusion on mitochondrial function, particularly in the context of disease, are not known. Limited evidence suggests that mitochondria may be involved in the pathogenesis of pulmonary hypertension and asthma, where increased cell proliferation, defective apoptosis and a shift in energy production pathways have been observed (30,31). Mitochondrial contribution to COPD has also been reported (13,24,32).

There is evidence that exposure to CS is connected to an increased risk in the development of asthma and exacerbation of asthma symptoms (6,7,33,34). While a multitude of cell types in the airway can mediate CS effects and participate in asthma development, we focused on ASM cells for a number of reasons: i) they play a crucial role in airway contractility (35–38); ii) they produce and respond to agents involved in inflammation and hyperresponsiveness (37–47), both of which are hallmarks of an asthmatic airway; and iii)

increase in ASM proliferation and remodeling has been identified as a major aspect of airway narrowing in asthma (35,37,41,42,46–49). Towards exploring ASM mitochondrial contribution to asthma, in an earlier study, we assessed the effect of cigarette smoke extract (CSE) on mitochondrial morphology in primary ASM cells (28). Our results demonstrated that CS increases mitochondrial fission in ASM cells (by upregulating the expression fission protein Drp1 and suppressing the expression of the fusion protein Mfn2), CS exposure elevates ROS (reactive oxygen species) production (by enhancing mitochondrial fission), exposure to CS causes a reduction in ATP production, and in asthmatic ASM cells, mitochondria are highly fragmented even under control conditions with CS worsening fragmentation (28). These results led us to reason that by disrupting mitochondrial networks and augmenting ROS generation in ASM cells, CS may profoundly impact mitochondrial function, thus predisposing the airway to development of asthma. Accordingly, the premise of the current study is that CS-induced changes in mitochondrial morphology evoke quantifiable changes in mitochondrial function in the ASM.

In the present study, we induced mitochondrial fragmentation in primary ASM cells using 1% CSE with or wihout concurrent inhibition of Mfn2 or of Drp1, and examined its effects on energy metabolism, cell proliferation and apoptosis. We complemented *in vitro* studies with an *in vivo* mouse model of chronic CS exposure and assessed, via laser capture microdissection (LCM), the expression of proteins involved in mitochondrial function.. Our results show that chronic exposure to CS does indeed have a pronounced effect on ASM cells and that it regulates the expression of gene products that play critical roles in mitochondrial function. We conclude that CS treatment severely impacts both the structure and function of ASM mitochondria, and that upsetting the balance between mitochondrial fission and fusion may be a mechanism underlying the increased ASM proliferation observed during asthma.

Materials and Methods

Materials

Small interfering RNAs (siRNAs) against Drp1 and Mfn2 siRNA were purchased from Ambion-Applied Biosystems (Austin, TX). Antibodies against Cyclin D1, PCNA (proliferating cell Nuclear Antigen), Caspase3, Caspase9, CytC (Cytochrome C), ATP5A (Mitochondrial ATPase α chain) and SDHA (Succinate Dehydrogenase Subunit A) were obtained from Santa Cruz Biotechnologies (Santa Cruz, CA). Antibodies against Enolase and LDHA (Lactose Dehydrogenase subunit A) were purchased from ProteinTech (Rosemont, IL). Antibodies to Bcl2 were obtained from Abcam (Cambridge, MA), and β-Actin antibodies from Sigma Aldrich (St. Louis MO). Culture plates, chemical reagents and cartridges for the XF^{e}24 Extracellular Flux Analyzer were purchased from SeaHorse Biosciences (Billerica, MA). TMRE and MitoTracker Green dyes, and CyQuant NF Kit was obtained from Invitrogen/ Molecular Probes (Carlsbad, CA). Multiparameter Apoptosis Kit was obtained from Cayman Chemicals (Ann Arbor, MI). Oligonucleotides used as primers in quantitative PCR were synthesized by Integrated DNA Technologies (Coralville, IA). Other chemicals [including 3-Bromopyruvate (3-BP)] were purchased from Sigma Aldrich (St. Louis MO), unless stated otherwise.

ASM cells

Isolation of human ASM cells by enzymatic dissociation has previously been described (59–61). Briefly, 3rd–6th level bronchi were isolated from surgical samples of lung resections incidental to patient thoracic surgery at Mayo Clinic Rochester, MN (all protocols approved by Institutional Review Board and considered 'minimal risk'; tissues were never obtained just for research purposes, but were collected from surgical pathology following tissue diagnosis). Studies were conducted only on ASM cells from patients confirmed as non-smokers based on their medical histories in order to exclude confounding effects of long-term smoke exposure on *in vitro* CS experiments. Following tissue collection, epithelium was removed, ASM dissected, immersed in ice-cold HBSS (Hanks' Balanced Salt Solution; 2 mM Ca^{2+}) and cells isolated as described previously (59–61). Cells were limited to ≤3 passages of subculture and were serum-deprived at least for 24 h prior to all experiments. ASM phenotype was frequently verified by expression of smooth muscle markers (actin and myosin, Ca^{2+} channel regulatory proteins such TRPC3, CD38 and Orai1), and by the lack of expression of epithelial and fibroblast markers as previously described (59,61).

CSE preparation

An aqueous solution of cigarette smoke extract (CSE) was prepared as previously described (62) using a modification of the Blue and Janoff method (63) via a smoking apparatus (50ml plastic syringe with a three-way stopcock), attached to a Kentucky 1RF4 cigarette and a sterile plastic tip. The CSE solution was sterile-filtered and used immediately. Analysis of nicotine and other metabolite concentrations in CSE has been reported previously (62). 1% CSE (diluted in serum-free medium) was used for all experiments based on our previous study (28).

Transfection with siRNAs

ASM cells were transfected with 200 pM siRNA against Drp1 or Mfn2 under serum- and antibiotic-free conditions, using Lipofectamine (Invitrogen, Carlsbad, CA), as described previously (28). 'Vehicle-alone' treatment and transfection with non-targeting RNA served as controls.

Mitochondrial morphology imaging and quantification

ASM cells in 8-well Lab-Teks were washed with 2mM Ca^{2+} HBSS (pH 7.4), loaded with 400nM MitoTracker Green (room temperature, 5 min) and visualized under a Nikon Eclipse Ti imaging system using a 100×/1.45 NA Nikon Plan Apo λ lens, an LED fluorescence light source and 16-bit high-sensitivity CCD camera. A single cell was isolated within images by creating masks (NIH ImageJ software), following correction for background fluorescence. Mitochondria were identified, via edge detection, using a MATLAB script for thresholding. Area-weighted averages of mitochondrial Form Factor and Aspect Ratio in each cell were calculated using the procedures developed by Koopman and colleagues (64,65)

Measurement of mitochondrial respiration and glycolysis

Approximately 100,000 ASM cells were seeded onto each well of 24-well XF-24 plates (SeaHorse Biosciences, Billerica, MA), in DMEM (Invitrogen, Carlsbad, CA). After 6–8h,

cells were transfected with siRNA and 24h later exposed to CSE for an additional 24h. Oxygen Consumption Rate (OCR; an indicator of mitochondrial respiration) was measured using an XF^{e}24 Extracellular Flux Analyzer (SeaHorse Biosciences) via manufacturer's protocol. Measurements were performed in the presence of 10mM glucose and the following inhibitors: 9μM Oligomycin (ATP uncoupler), 0.3μM FCCP (carbonyl cyanide p-trifluoromethoxyphenylhydrazone; accelerates electron transport chain), and 11μM Antimycin A (a Complex III inhibitor) with 11μM rotenone (a Complex I inhibitor), allowing for determination of basal respiration, ATP production, Maximal Respiration and Spare Respiratory Capacity. Values were normalized for total protein measured *post hoc*. For Extracellular Acidification Rate (ECAR; an indicator of glycolysis), cells were treated as stated previously, but were exposed to 10mM glucose, 3μM Oligomycin and 100mM 2-Deoxy Glucose. Glycolysis, glycolytic capacity and glycolytic reserve were measured and normalized for total protein *post hoc* (66,67).

Mitochondrial Membrane Potential (MMP)

ASM cells were transfected with siRNA against Drp1 or Mfn2 and exposed to either culture medium or 1% CSE for 48h. Mitochondrial membrane potential was measured using 50nM TMRE (Tetramethyl rhodamine ethyl ester), with cells visualized on the Nikon Eclipse Ti imaging system (as above) using a 20×/ 0.75M 1mm DIC N2 lens. Active, intact mitochondria readily take up the fluorescent dye (68,69).

CyQuant Cell Proliferation Assay

Proliferation of ASM cells based on DNA content was measured as described previously (70). Briefly, ASM cells were grown in 96-well plates (~5,000 cells/ well), serum-deprived, transfected with siRNA, exposed to 1% CSE for 48h and incubated with CyQuant NF (Invitrogen) for 30 min. Dye (CyQuant) binding to DNA (fluorescence) was measured on a FlexStation3 microplate reader (Molecular Devices, Sunnyvale, CA). Dye calibrations and normalization were performed, as previously described (70).

Apoptosis

ASM cells were grown in 96-well plates (~5,000 cells/ well), serum-deprived, transfected with siRNA, and exposed to 1% CSE for 48h. Apoptosis was assayed using the Multiparameter Apoptosis Kit (Cayman Chemicals) which measures MMP (TMRE fluorescence), cell number (Hoechst dye fluorescence) and apoptosis (Annexin V-FITC fluorescence). All fluorescence readings were performed on a FlexStation3 microplate reader (TMRE fluorescence: excitation/ emission= 560/ 595 nm; Annexin V-FITC fluorescence: excitation/ emission= 485/ 535 nm; T Hoechst dye: excitation/ emission= 355/ 465 nm).

In vivo CS exposure in mice

Animal procedures were approved by the Mayo Clinic Institutional Animal Care and Use Committee and adhered to the guidelines of the American Physiological Society. Wild-type C57BL6 adult mice (Jackson Laboratories, Bar Harbor, Maine) were exposed to CS using a Teague TE-2 System (Teague Enterprises, Woodland, CA) (71). Mice were exposed to

regulated concentrations of CS generated from 2 cigarettes every 10 min for a total of 3 h/day, 5 days/week, and for 6 weeks. CS inhalation was monitored by measuring serum nicotine levels at the time of sacrifice (71,72).

Histological analyses

Standard protocols were used for hematoxylin and eosin (H&E) and Masson Trichrome (Polysciences Inc., Warrington PA) staining of 5μm lung sections. Following staining procedures, slides were visualized and images acquired using an Olympus Axioplan2 microscope at a magnification of 200×.

Laser capture microdissection and PCR analysis

After completion of the long-term CS exposure regimen animals were overdosed with pentobarbital, lungs inflated with air (25 cm H_2O) via tracheal cannulation and rapidly frozen under RNase-free conditions (73). Lungs from at least 4 animals per group were isolated and cryosectioned at 10μm under RNase-free conditions, and an Arcturus XT microdissection system (Molecular Devices, Sunnyvale, CA) used to microdissect epithelium vs. ASM from small airways (300–350 μm diameter), as described previously (73). Total RNA (4 caps/animal) was isolated and cDNA synthesized using standard techniques, with ribosomal protein S16 as internal control. Real-time PCR was performed in duplicates per cDNA template, and data for all cDNAs in a category (non-smoker vs. smoker mice) pooled for statistical analysis. All PCR reactions went through 65 amplification cycles. The ratio of fold change in expression of mRNA of interest was calculated by normalization of cycle threshold [C(t)] values of target genes (CyclinD1, Bcl2, PCNA, Caspase9, Cytochrome C, SDHA and ATP5A) to the reference gene (S16) using the comparative C(t) (ΔΔC(t)) method. Data are reported as ΔC(t) and the average ratio of fold change in mRNA of interest corrected for reference gene. Unexposed control was used as the calibrator for quantification. Primer sequences are listed in Table 1.

Q-PCR on cDNAs from ASMs

ASM cells were treated with 1% CSE for 48 h and total RNA isolated using RNeasy mini kit (Qiagen, Valencia, CA). Complementary DNA (cDNA) was prepared using the Transcriptor reverse transcription kit (Roche, Indianapolis, IN), and was used as a template for RT-PCR optimized for the Roche LC480 Light Cycler, with S16 as internal control. The ΔΔC(t) method as above was used to determine changes in expression of mRNA of interest. Unexposed control was used as the calibrator for quantification. Primers used for RT-PCR are listed in Table 2.

Immunoblotting

Standard Western blot techniques were used to determine changes in protein levels in whole ASM cell lysates and quantification performed on a Li-Cor Odyssey IR scanning system (Lincoln, NE). Band intensities were normalized against β-Actin. Extracts from at least 4 ASM populations were used for each experiment.

Statistical Analysis

All experiments were performed in quadruplicate using different sets of ASM cells isolated from at least 4 different individuals. Controls represent cells not exposed to CSE or those not transfected. For LCM, at least 4 animals per group were used, and 4 caps were obtained per animal. Comparisons were made using independent Student's *t*-test or two-way ANOVA as appropriate. Bonferroni correction was used for repeated comparisons. Statistical significance was tested at the $P<0.05$ level. Values are reported as means ± SE. "N" values representing numbers of individuals are provided in the figure legends.

Results

We have previously shown that exposure to CSE induces substantial fragmentation in human ASM mitochondria. In addition, CS upregulates the expression of Drp1 (a cytoplasmic protein involved in mitochondrial fission) while reducing the expression of Mfn2 (a mitochondrial outer membrane protein involved in mitochondrial fusion). Furthermore, CS-triggered changes in ASM mitochondrial morphology are mediated by increased ROS production and a variety of intracellular signaling pathways (28). The present study builds on those observations and tests if the regulation of mitochondrial morphology leads to alterations in mitochondrial function. First, we verified the effects of altering Drp1 or Mfn2 level on mitochondrial morphology in untreated and CS-exposed ASM cells by using siRNAs. Efficacy of these siRNAs was previously tested and reported (28). As shown in Figure 1A, the long and networked mitochondrial tracks seen in untreated cells are no longer visible after CS treatment, where the mitochondria appear highly fragmented. Inhibition of Drp1 by siRNA results in a 'hyperfused' morphology, where mitochondrial tracks are longer and more networked than untransfected ('Vehicle Only') cells. When Mfn2 expression is blocked, however, mitochondrial fragmentation increases, even in the absence of CSE. These results are quantified by Form Factor and Aspect Ratio, parameters that reflect the complexity of mitochondrial morphology. Inducing fragmentation via exposure to CS or inhibiting Mfn2 dramatically reduces both Form Factor and Aspect Ratio in ASM cells (Figures 1B and 1C). These data clearly indicate essential roles for Drp1 and Mfn2 in mitochondrial fission and fusion, respectively. Thus, subsequent assays on the functional consequences of fission-fusion imbalance were performed in the context of altered Drp1 or Mfn2 expression.

In experiments measuring bioenergetic function of mitochondria in ASM cells inhibiting the fission protein Drp1 resulted in significant reduction in basal respiration, decreased ATP generation and lower spare reserve capacity of ATP production (Figure 2A, summarized in Figure 2B). Conversely, baseline respiration, ATP generation and capacity were elevated when Mfn2-dependent fusion was inhibited (Figure 2A, 2B).

We previously demonstrated that exposing ASM cells for 24h to CSE markedly decreases baseline respiration and mitochondrial ATP production (28). Consistent with this our current investigation showed lower OCR readings in CSE-exposed ASM cells (Figure 2A). However, we had also previously shown that CSE increases Drp1 (inducing mitochondrial fission) and decreases Mfn2. Therefore, in the current study we expected Drp1siRNA to reverse CSE effect on OCR readings. However, CSE effects on OCR parameters were

largely unaffected by Drp1siRNA. In contrast, Mfn2 siRNA partly reversed CSE effects on OCR parameters, but did not enhance these parameters to the extent seen in unexposed cells (Figure 2B).

One of the factors that determine the bioenergetic capacity of mitochondria is the availability of electron transport chain (ETC) enzymes. To test if altered expression of ETC proteins influences mitochondrial morphology and respiration during CS exposure, we exposed ASM cells transfected with Drp1 or Mfn2 siRNA to 1% CSE and examined the expression of succinate dehydrogenase subunit A (SDHA; an inner mitochondrial membrane enzyme that participates in the citric acid cycle and respiratory chain). Drp1siRNA significantly reduced SDHA mRNA levels, while Mfn2siRNA increased SDHA levels (Figure 3A). Exposure to CSE also reduced SDHA expression, an effect partly reversed by Mfn2 inhibition (Figure 3A). A similar pattern of expression was seen with SDHA protein (Figure 3B). It should be noted here that we also examined a second ETC protein, ATP synthase alpha subunit 1 (ATP5A; an inner mitochondrial membrane, complex V enzyme), and found comparable effects at both mRNA (Table 3) and protein (Table 4) levels.

Mitochondrial membrane potential is known to directly affect mitochondrial function (74,75) and perturbing the mitochondrial networking system (i.e., fission-fusion balance) has been shown to profoundly regulate MMP (76,77). Accordingly, we tested the effect of CS on MMP by exposing ASM cells to 1% CSE for 48h and then visualizing mitochondrial integrity using the dye TMRE. This cell-permeant, fluorescent dye is readily sequestered by active mitochondria (i.e., mitochondria with intact MMP). Untransfected cells and those transfected with Drp1siRNA have robust TMRE florescence, while Mfn2siRNA-transfected cells show diminished fluorescence (Figure 4). Increasing mitochondrial fragmentation by CS also results in a comparable loss of MMP (Figure 4), suggesting that mitochondrial morphology may be an important predicator for mitochondrial membrane integrity and mitochondrial function in ASM.

Mitochondria play a major role in maintaining cellular homeostasis by regulating the balance between cell proliferation and cell death (apoptosis) (11,78–83). In this regard, altered energy production has commonly been implicated in dysregulation of cell division (15–18). This prompted us to investigate the outcome of CS-induced changes in mitochondrial morphology in terms of cell proliferation and apoptosis. We previously observed an increase in ASM proliferation following 1% CSE exposure (37), and confirmed this in the current study (Figure 5A). Additional experiments show that Drp1siRNA inhibits proliferation while Mfn2 siRNA elevates ASM proliferation, both in the absence and presence of CSE (Figure 5A). These functional effects were corroborated at a molecular level, by changes in the expression of the marker proliferating cell nuclear antigen (PCNA) mRNA (Figure 5B) and protein (Figure 5C). We also examined Cyclin D1 and Bcl2 and found consistent changes in mRNA and protein (Tables 3 and 4).

In order to determine whether CS has a reciprocal effect on ASM apoptosis, we used a multi-parameter assay. Our results indicate that exposure to CS reduces apoptosis in ASM (Figure 6A). While Drp1 suppresses apoptosis, Mfn2 seems to promote it. This result was further supported by measuring the expression of Caspase9, an enzyme involved in the

apoptotic cascade. We found that CSE downregulated Caspase9 at both transcriptional (Figure 6B) and protein (Figure 6C) levels. Drp1 siRNA elevated Caspase9 mRNA and protein, whereas blocking Mfn2 had the opposite effect. Similar trends were observed for other apoptotic markers Caspase3 (Supplemental Figure 1) and cytochrome C (CytC; Tables 3 and 4). Experiments in ASM conducted with apoptosis inducers Embelin and Apoptozole resulted in increased expression of Caspase 3 and 9, an effect counteracted by CS (Supplemental Figure 2)..

Our data suggest that CS-induced changes in mitochondrial fission-fusion parameters influence mitochondrial function (i.e., cellular energetics and cell fate determination). Although the relationship between Drp1 and Mfn2 is not necessarily reciprocal [despite our observations that CS increases Drp1 expression and mitochondrial fission (28), Drp1 knockdown increases Mfn2 expression in ASM cells (our unpublished data) and enhances cell proliferation], CS actually reduces OCR parameters rather than increasing ATP availability for such a proliferative state. It is possible that CS redirects energy metabolism in such a way that the decline in oxidative mitochondrial function is compensated, while a proliferative phenotype is still favored. Such a scenario is possible if the cells use glycolysis as their primary source of ATP, rather than the more efficient oxidative phosphorylation. This switch has been commonly observed in several tumor cells (Warburg effect), and CS has been shown to induce it (84–86). To determine the effect of CS on glycolysis ASM cells were exposed to 1% CSE in the presence or absence of siRNA against Drp1 or Mfn2. We observed a significant increase in ECAR (extracellular acidification rate; indicative of robust glycolysis), when cells were exposed to CSE, or when Mfn2 was inhibited, while blunting fission reduced the glycolytic rate (Figure 7A). Glycolytic capacity and glycolytic reserve, two other aspects of ECAR, were also observed to increase when fission was induced, either by CSE or Mfn2 inhibition (Figures 7B and 7C). To check if this increase in glycolysis was due to a change in the expression of glycolytic enzymes, we quantified the level of Enolase, the enzyme that catalyzes the interconversion of 2-phosphoglycerate to phosphoenolpyruvate during late stage glycolysis. Enolase expression is elevated in CS-exposed cells as well as Mfn2 siRNA-transfected cells, not only providing a possible explanation for the increase in ECAR rates, but also suggesting a correlation between mitochondrial morphology regulation and glycolysis-dependent energy production (Figure 7D). The latter notion is further strengthened by our observation that ASM proliferation is significantly affected by inhibiting glycolysis. Additional experiments with ASM cells transfected with siRNAs against Drp1 or Mfn2 and treated with 100μM 3-BP (3-bromopyruvate), a hexokinase inihbitor, shows 3-BP causes a reduction in ASM proliferation in untransfected cells; proliferation is further decreased in the cells where fission is blocked via Drp1siRNA (Figure 7E). Exposure to CSE seems to compensate for this effect, suggesting that: i) regulation of glycolysis is tied to ASM proliferation, and, ii) agents that disrupt mitochondrial fission- fusion equilibrium (such as CSE and Drp1/ Mfn2 siRNAs) may regulate mitochondria-mediated ASM proliferation by interfering with the glycolytic pathway.

To contextualize the *in vitro* (human ASM) data, and to address the issue of whether mitochondrial fission-fusion cycle and the bioenergetics in the ASM actually contribute to CS effects *in vivo*, we evaluated ASM mitochondria in mice exposed to room air vs. CS for

six weeks. Lung function in CS-exposed mice was impaired, as evidenced by increased resistance and decreased compliance in response to methacholine stimulation (data not shown). Histological analyses (H&E and Masson-Trichrome) show significant thickening (suggestive of increased ASM mass) and fibrosis in the airways exposed to CS (Figure 8). We studied the expression of proteins involved in proliferation, apoptosis, and mitochondrial oxidative phosphorylation, using LCM-based mRNA analysis on the ASM layer isolated from the airways of these mice. We found significant differences in gene expression patterns in CS-exposed airways compared to unexposed airways (Figure 9). Expression of proliferation markers such as PCNA, CyclinD1 and Bcl2 increased in CS-exposed airways, while apoptosis proteins CytC and Caspase-9 were downregulated (Figures 9A and B). CS also blunted the expression of ETC proteins SDHA and ATP5A (Figure 9C). Additionally, we performed LCM-based PCR analysis of airway epithelial layers from the same animals and found the changes in expression of the same genes comparable to those seen with the ASM layer (data not shown). The marked and consistent changes in mRNA expression observed in the ASM layer as well as the epithelial layer suggest that the effects of chronic CS exposure directly influence ASM cells

Discussion

Environmental factors such as cigarette smoke contribute to airway diseases including asthma. In asthma, altered cell proliferation and airway remodeling are key features. Thus, understanding the mechanisms by which CS affects airway cells, causing structural and functional changes in lung disease becomes vital. The current study makes several novel contributions by establishing a link between mitochondrial morphology and mitochondrial function in ASM cells, in terms of changes in oxidative phosphorylation vs. glycolysis, as well as global cellular functions in the context of CS exposure in vivo.

Our quantification of mitochondrial bioenergetic function highlights the importance of the integrity of mitochondrial networks in energy production. Regulation of mitochondrial morphology by oxidative phosphorylation has been reported in skin fibroblasts (87). Although this study examined networked vs. fragmented mitochondria, it did not extend the analysis to individual proteins involved in mitochondrial fission vs. fusion. The present study dissects the relationship between mitochondrial morphology and oxidative phosphorylation, demonstrating that blocking fission (by Drp1siRNA) reduces energy metabolism, while inhibition of fusion (via Mfn2siRNA) enhances ATP generation in the airway. The former finding is consistent with what has been previously shown in HeLa cells (88).

Previously, we demonstrated that CS is a potent inducer of mitochondrial fission in human ASM cells (28). Our present study suggests that CS-induced changes in mitochondrial fission-fusion parameters influence mitochondrial function (i.e., cellular energetics and cell fate determination). However, the relationships between Drp1 vs. Mfn2 and CS effects on OCR are not entirely reciprocal: although CSE increases Drp1 and mitochondrial fission (28), and enhances cell proliferation, we found that CS actually reduces OCR parameters rather than increasing ATP availability, which would be required for a proliferative state. One obvious explanation is CS cytotoxicity. However, we did not observe increased cell

death due to CS treatment; in fact, our results show an increase in proliferation as a result of CS exposure. Thus, even though there is an elevated demand for ATP production (due to CS-induced stress), mitochondria are unable to supply the required energy through oxidative phosphorylation. One potential reason, as we have shown here, is that there is an anomalous expression of proteins involved in ATP synthesis via ETC. Alternatively (but not mutually exclusively), ROS generated through CS modify ROS scavengers (antioxidant enzymes such as GSH, for example), which in turn leads to decreases in ATP synthesis and reserve capacity. We did not specifically explore ROS in this study, but this phenomenon has been observed in aortic smooth muscle cells (89). Even though normal ETC activity results in ROS generation, cellular antioxidant mechanisms balance it out, thereby averting significant cellular damage. Conversely, disrupting mitochondrial function by inhibiting ETC complexes increases ROS production, thereby overwhelming cellular ROS scavenging systems (90). There is increasing evidence signifying the link between mitochondrial function and the pathogenesis of airway diseases. For example, decreased mitochondrial function, consequential to blocking ETC and increased ROS production have been observed in the lungs of COPD patients (91), and NADPH oxidase has been identified as a causative agent for allergic airway inflammation (92).

An intriguing result from our study is the change in SDHA expression. This subunit of Complex II of the respiratory chain has been reported to act as a tumor suppressor (93,94). On the other hand, its expression has also been shown to increase in certain invasive tumors (95). In line with our proliferation data, CS seems to downregulate SDHA expression, suggesting that SDHA may be anti-proliferative; however, inhibition of Drp1, which is pro-proliferative, also decreases SDHA expression. While this discrepancy requires further exploration, previous studies in smooth muscle cells suggest that ROS signaling is a plausible mechanism that controls SDHA expression (96).

Spare respiratory capacity is the extra mitochondrial capability utilized by a cell under extreme stress, and is thought to be vital for long-term cell survival (97–100). CS depletion of reserve capacity may thus indicate ASM response to environmental stress, where mitochondria are forced to use unconventional metabolites as energy sources (100,101). The resultant changes in mitochondrial properties such as membrane potential may promote the proliferative phenotype seen with CS exposure. In this context, it is important to understand the recently introduced concept of Bioenergetic Health Index (BHI) (102). BHI represents an individual’s mitochondrial bioenergetic profile for a specific cell type, and is calculated based on observations that i) the reserve capacity is higher when the mitochondria are healthy than when the cellular demand becomes high enough to cause mitochondrial dysfunction (high energy demand depletes the reserve capacity), and that ii) conditions that cause mitochondrial dysfunction lead to an increase in proton leak (thus reducing ATP production), and in non-mitochondrial respiration (such as ATP generation by glycolysis). We found these assumptions to be true when we compared OCR in CS-exposed ASM cells to controls: CS exposure caused an increase in proton leak and non-mitochondrial respiration (data not shown). Interestingly, we also found that the BHI value in CS-treated cells was lower (mean 1.28 ± SE 0.12) than untreated cells (mean 8.294 ± SE 0.685). Thus, it is possible that quantification of bioenergetics directly represents the extent of metabolic stress on a specific tissue/ cell type.

Another major observation in our study was that the loss of balance between mitochondrial fission and fusion shifts the source for ATP synthesis from oxidative phosphorylation to glycolysis. This phenomenon is seen in tumors (103) and disease conditions such as pulmonary arterial hypertension (104,105). In vascular smooth muscle cells, PDGF-induced proliferation is accompanied by a dramatic increase in both glycolytic flux and mitochondrial oxygen consumption (16). In ASM cells, however, we find that agents such as CS that promote mitochondrial fission, while suppressing ATP production, increase glycolysis. This distinct trend (i.e., increased glycolytic rate with a concomitant reduction in ATP production) was also observed to occur in epithelial cells from CS-exposed esophagus (86). Similarly, a decrease in respiration has been observed in CS-exposed mouse alveolar cells, along with altered glycolysis, and increased palmitate utilization (84). This shift may explain how the increased ATP demand in CS-exposed ASM cells is met, and allows for proliferation and cellular survival. In this regard, it is important to point out that our observations of a shift towards glycolysis are unlikely to be specific to human ASM cells *per se*, since we observe comparable changes in ETC proteins in the CS-exposed mouse lung. Here, it is important to note that earlier studies in whole mouse lung showed that chronic CS exposure reduces glycolysis and upregulates ETC genes (85), i.e. in contrast to our observations, and the study by Kim et al. in other cell types (86). The reasons underlying these discrepancies are not clear. What seems more obvious is that influencing mitochondrial morphology via CS might subsequently affect a variety of mitochondrial mediated cellular functions. Interestingly, Enolase, has been used as a diagnostic marker for certain tumors (106–109). Similarly, an overabundance of LDHA (Lactate dehydrogenase subunit A) has also been observed in many tumors (110–113). Our data (Table 4) show the expression of LDHA following the same trend as Enolase. An increase in LDHA expression may diminish the amount of pyruvate entering the mitochondria for oxidative phosphorylation, thus blunting mitochondrial bioenergetic function.

CS regulation of cell fate (proliferation vs. apoptosis) is likely dependent on various factors including cell type, duration of exposure and the parameters examined. For instance, when hepatocytes were exposed to acrolein (an aldehyde pollutant and major component of CS), ATP levels are depleted, but cells undergo robust apoptosis (114). CS exposure has also been found to evoke release of ceramides (proapoptotic lipids) in lung, upstream of mitochondrial dysfunction (115). However, increased proliferation and reduced apoptosis upon exposure to CS (116) or polycyclic aromatic hydrocarbons (117) have been reported in bronchial epithelial cells. Altered energy metabolism seen following CS exposure of stromal fibroblasts seems to drive a tumorigenic phenotype in neighboring epithelial cells (118). It has been shown, at least in the case of lung fibroblasts, that sensitivity to CS may depend on individual variations among cell populations (119). In the present study, CS acts as a pro-proliferative agent in both epithelium (at least in mice) and ASM, and this effect seems to be mediated via mitochondrial fragmentation. The relevance of this finding becomes significant in light of what is known about airway diseases: increased CyclinD1 expression and PKC activity, associated with increased proliferation is observed in asthmatic ASM (120). Similarly, increased proliferation, resistance to apoptosis, decreased ATP production and a switch to glycolysis are seen in severe pulmonary hypertension (30).

Specific roles of the fission protein Drp1 as a proliferation promoter and the fusion protein Mfn2 as a proliferation suppresser have been proposed earlier: Drp1 inhibition increases apoptosis (15,83,121–124), while Mfn2 enhances vascular smooth muscle apoptosis via Akt phosphorylation, increased Caspase9 expression and CytC release (80,81). Our results are consistent with these reports. Indeed, we previously dissected the cytosolic (MAPK/ ERK, PI3K/ Akt1 and PKC) and nuclear (NFκB and Nrf2) signaling pathways that regulate Drp1 and Mfn2 expression, in the context of CS exposure (28). Interestingly, these pathways play major roles in mediating cell proliferation, prompting us to speculate that at the molecular level, CS regulates the association between mitochondrial morphology and function by modulating these signaling mechanisms.

Another possible trigger for a proliferative cell phenotype is autophagy (125,126). Several mechanisms, including ROS signaling, enhanced cell survival through active recycling of the cytoplasmic cargo, regulation of lipid and glycogen metabolism, changes in mitochondrial structure and dynamics, and mediation of inflammatory signaling, have been speculated to lead to autophagy-promoted proliferation (19,122,127–131). Autophagic degradation of mitochondria (mitophagy) has recently garnered significant attention for its vital role in cell fate determination and in cellular responses to energy requirements (125,132,133), and could contribute to a number of diseases (130,131,134–137). Unpublished data from our lab indicate that an increase in mitochondrial fission, either via exposure to CS or by abrogating fusion protein expression, induces autophagy in ASM. Thus, it is possible that enhanced proliferation intensifies metabolic demands, forcing the cell to recycle its resources through autophagy in order to meet these demands.

Finally, our *in vivo* data validate the notion that in the airway, the ASM (in addition to the epithelium, which first experiences CS) is a major target for CS effects. Several recent studies have shown that long-term exposure to CS damages the epithelium and its barrier function (50–57), i.e., the ASM layer can be exposed to CS directly. In addition, in response to CS exposure, the epithelium produces factors that can influence adjoining ASM tissue (58). Thus, with the high likelihood that CS effects on ASM are relevant, we show that the ASM layer is prone to CS-induced modulation of gene expression, especially with regard to those involved in mitochondrial function such as energy metabolism, proliferation, and apoptosis, as summarized in the proposed model (Figure 10). We conclude that CS treatment severely impacts both the structural and functional aspects of ASM mitochondria, and that upsetting the balance between mitochondrial fission and fusion may be a mechanism underlying the increased ASM proliferation seen during asthma.

Supplementary Material

Refer to Web version on PubMed Central for supplementary material.

Acknowledgments

Supported by Young Clinical Scientist Award (Aravamudan) and Clinical Innovator (Vassallo) Grants from the Flight Attendants Medical Research Institute, and R01 grants from the National Institutes of Health [HL126451 (Sieck, Prakash), HL056470 (Prakash), and HL088029 (Prakash)].

References

1. Eisner MD. Environmental tobacco smoke and adult asthma. Exp Lung Res. 2005; 31(Suppl 1):8–14. [PubMed: 16395853]
2. Feinson JA, Chidekel AS. Adult smoking and environmental tobacco smoke: a persistent health threat to children. Del Med J. 2006; 78:213–218. [PubMed: 16821557]
3. Lodrup Carlsen KC, Jaakkola JJ, Nafstad P, Carlsen KH. In utero exposure to cigarette smoking influences lung function at birth. Eur Respir J. 1997; 10:1774–1779. [PubMed: 9272918]
4. Omini C, Hernandez A, Zuccari G, Clavenna G, Daffonchio L. Passive cigarette smoke exposure induces airway hyperreactivity to histamine but not to acetylcholine in guinea-pigs. Pulm Pharmacol. 1990; 3:145–150. [PubMed: 2135217]
5. Thomson NC. The role of environmental tobacco smoke in the origins and progression of asthma. Curr Allergy Asthma Rep. 2007; 7:303–309. [PubMed: 17547853]
6. Walker B Jr, Stokes LD, Warren R. Environmental factors associated with asthma. Journal of the National Medical Association. 2003; 95:152–166. [PubMed: 12760611]
7. Weiss ST, Utell MJ, Samet JM. Environmental tobacco smoke exposure and asthma in adults. Environmental health perspectives. 1999; 107(Suppl 6):891–895. [PubMed: 10592149]
8. Chan DC. Mitochondria: dynamic organelles in disease, aging, and development. Cell. 2006; 125:1241–1252. [PubMed: 16814712]
9. Chan DC. Mitochondrial fusion and fission in mammals. Annu Rev Cell Dev Biol. 2006; 22:79–99. [PubMed: 16704336]
10. Chan DC. Fusion and fission: interlinked processes critical for mitochondrial health. Annu Rev Genet. 2012; 46:265–287. [PubMed: 22934639]
11. Liesa M, Palacin M, Zorzano A. Mitochondrial dynamics in mammalian health and disease. Physiol Rev. 2009; 89:799–845. [PubMed: 19584314]
12. Youle RJ, van der Bliek AM. Mitochondrial fission, fusion, and stress. Science. 2012; 337:1062–1065. [PubMed: 22936770]
13. Hoffmann RF, Zarrintan S, Brandenburg SM, Kol A, de Bruin HG, Jafari S, Dijk F, Kalicharan D, Kelders M, Gosker HR, Ten Hacken NH, van der Want JJ, van Oosterhout AJ, Heijink IH. Prolonged cigarette smoke exposure alters mitochondrial structure and function in airway epithelial cells. Respir Res. 2013; 14:97. [PubMed: 24088173]
14. Willems PH, Smeitink JA, Koopman WJ. Mitochondrial dynamics in human NADH:ubiquinone oxidoreductase deficiency. The international journal of biochemistry & cell biology. 2009; 41:1773–1782. [PubMed: 19703648]
15. Mitra K, Wunder C, Roysam B, Lin G, Lippincott-Schwartz J. A hyperfused mitochondrial state achieved at G1-S regulates cyclin E buildup and entry into S phase. Proc Natl Acad Sci U S A. 2009; 106:11960–11965. [PubMed: 19617534]
16. Perez J, Hill BG, Benavides GA, Dranka BP, Darley-Usmar VM. Role of cellular bioenergetics in smooth muscle cell proliferation induced by platelet-derived growth factor. Biochem J. 2010; 428:255–267. [PubMed: 20331438]
17. Schieke SM, Ma M, Cao L, McCoy JP Jr, Liu C, Hensel NF, Barrett AJ, Boehm M, Finkel T. Mitochondrial metabolism modulates differentiation and teratoma formation capacity in mouse embryonic stem cells. J Biol Chem. 2008; 283:28506–28512. [PubMed: 18713735]
18. Schieke SM, McCoy JP Jr, Finkel T. Coordination of mitochondrial bioenergetics with G1 phase cell cycle progression. Cell Cycle. 2008; 7:1782–1787. [PubMed: 18583942]
19. Dhingra R, Kirshenbaum LA. Regulation of mitochondrial dynamics and cell fate. Circ J. 2014; 78:803–810. [PubMed: 24647412]
20. Lennon FE, Salgia R. Mitochondrial dynamics: biology and therapy in lung cancer. Expert opinion on investigational drugs. 2014; 23:675–692. [PubMed: 24654596]
21. Mishra P, Chan DC. Mitochondrial dynamics and inheritance during cell division, development and disease. Nat Rev Mol Cell Biol. 2014; 15:634–646. [PubMed: 25237825]

22. Salabei JK, Hill BG. Mitochondrial fission induced by platelet-derived growth factor regulates vascular smooth muscle cell bioenergetics and cell proliferation. Redox biology. 2013; 1:542–551. [PubMed: 24273737]

23. Westrate LM, Sayfie AD, Burgenske DM, MacKeigan JP. Persistent mitochondrial hyperfusion promotes G2/M accumulation and caspase-dependent cell death. PLoS One. 2014; 9:e91911. [PubMed: 24632851]

24. Hara H, Araya J, Ito S, Kobayashi K, Takasaka N, Yoshii Y, Wakui H, Kojima J, Shimizu K, Numata T, Kawaishi M, Kamiya N, Odaka M, Morikawa T, Kaneko Y, Nakayama K, Kuwano K. Mitochondrial fragmentation in cigarette smoke-induced bronchial epithelial cell senescence. Am J Physiol Lung Cell Mol Physiol. 2013; 305:L737–L746. [PubMed: 24056969]

25. Meyer A, Zoll J, Charles AL, Charloux A, de Blay F, Diemunsch P, Sibilia J, Piquard F, Geny B. Skeletal muscle mitochondrial dysfunction during chronic obstructive pulmonary disease: central actor and therapeutic target. Experimental physiology. 2013; 98:1063–1078. [PubMed: 23377494]

26. Yoshida T, Tuder RM. Pathobiology of cigarette smoke-induced chronic obstructive pulmonary disease. Physiol Rev. 2007; 87:1047–1082. [PubMed: 17615396]

27. Aravamudan B, Delmotte P, Thompson M, Vassallo R, Sieck GC, Pabelick CM, Prakash YS. Response to letter by Dr. Marc Hershenson (exposure of airway smooth muscle cells to cigarette smoke extract). Am J Physiol Lung Cell Mol Physiol. 2014; 307:L346. [PubMed: 25128539]

28. Aravamudan B, Kiel A, Freeman M, Delmotte P, Thompson M, Vassallo R, Sieck GC, Pabelick CM, Prakash YS. Cigarette smoke-induced mitochondrial fragmentation and dysfunction in human airway smooth muscle. Am J Physiol Lung Cell Mol Physiol. 2014; 306:L840–L854. [PubMed: 24610934]

29. Mabalirajan U, Dinda AK, Kumar S, Roshan R, Gupta P, Sharma SK, Ghosh B. Mitochondrial structural changes and dysfunction are associated with experimental allergic asthma. J Immunol. 2008; 181:3540–3548. [PubMed: 18714027]

30. Fijalkowska I, Xu W, Comhair SA, Janocha AJ, Mavrakis LA, Krishnamachary B, Zhen L, Mao T, Richter A, Erzurum SC, Tuder RM. Hypoxia inducible-factor1alpha regulates the metabolic shift of pulmonary hypertensive endothelial cells. The American journal of pathology. 2010; 176:1130–1138. [PubMed: 20110409]

31. Reddy PH. Mitochondrial Dysfunction and Oxidative Stress in Asthma: Implications for Mitochondria-Targeted Antioxidant Therapeutics. Pharmaceuticals (Basel). 2011; 4:429–456. [PubMed: 21461182]

32. Ballweg K, Mutze K, Konigshoff M, Eickelberg O, Meiners S. Cigarette smoke extract affects mitochondrial function in alveolar epithelial cells. Am J Physiol Lung Cell Mol Physiol. 2014 ajplung 00180 02014.

33. Jaakkola MS, Jaakkola JJ. Assessment of exposure to environmental tobacco smoke. Eur Respir J. 1997; 10:2384–2397. [PubMed: 9387970]

34. Jackson DJ, Hartert TV, Martinez FD, Weiss ST, Fahy JV. Asthma: NHLBI Workshop on the Primary Prevention of Chronic Lung Diseases. Annals of the American Thoracic Society. 2014; 11(Suppl 3):S139–S145. [PubMed: 24754822]

35. Bao J, Sack MN. Protein deacetylation by sirtuins: delineating a post-translational regulatory program responsive to nutrient and redox stressors. Cellular and molecular life sciences : CMLS. 2010; 67:3073–3087. [PubMed: 20680393]

36. Sathish V, Freeman MR, Long E, Thompson MA, Pabelick CM, Prakash YS. Cigarette Smoke and Estrogen Signaling in Human Airway Smooth Muscle. Cellular physiology and biochemistry : international journal of experimental cellular physiology, biochemistry, and pharmacology. 2015; 36:1101–1115.

37. Sathish V, Vanoosten SK, Miller BS, Aravamudan B, Thompson MA, Pabelick CM, Vassallo R, Prakash YS. Brain-derived neurotrophic factor in cigarette smoke-induced airway hyperreactivity. Am J Respir Cell Mol Biol. 2013; 48:431–438. [PubMed: 23258230]

38. Smelter DF, Sathish V, Thompson MA, Pabelick CM, Vassallo R, Prakash YS. Thymic stromal lymphopoietin in cigarette smoke-exposed human airway smooth muscle. J Immunol. 2010; 185:3035–3040. [PubMed: 20660708]

39. Lee IK, Kang KA, Zhang R, Kim BJ, Kang SS, Hyun JW. Mitochondria protection of baicalein against oxidative damage via induction of manganese superoxide dismutase. Environmental toxicology and pharmacology. 2011; 31:233–241. [PubMed: 21787690]
40. Gavrila A, Chachi L, Tliba O, Brightling C, Amrani Y. Effect of the plant derivative Compound A on the production of corticosteroid-resistant chemokines in airway smooth muscle cells. Am J Respir Cell Mol Biol. 2015; 53:728–737. [PubMed: 25897650]
41. Gerthoffer WT. Migration of airway smooth muscle cells. Proc Am Thorac Soc. 2008; 5:97–105. [PubMed: 18094091]
42. Girodet PO, Ozier A, Bara I, Tunon de Lara JM, Marthan R, Berger P. Airway remodeling in asthma: new mechanisms and potential for pharmacological intervention. Pharmacology & therapeutics. 2011; 130:325–337. [PubMed: 21334378]
43. Hershenson MB, Brown M, Camoretti-Mercado B, Solway J. Airway smooth muscle in asthma. Annual review of pathology. 2008; 3:523–555.
44. Koziol-White CJ, Panettieri RA Jr. Airway smooth muscle and immunomodulation in acute exacerbations of airway disease. Immunol Rev. 2011; 242:178–185. [PubMed: 21682745]
45. Pearson H, Britt RD Jr, Pabelick CM, Prakash YS, Amrani Y, Pandya HC. Fetal human airway smooth muscle cell production of leukocyte chemoattractants is differentially regulated by fluticasone. Pediatr Res. 2015; 78:650–656. [PubMed: 26331770]
46. Royce SG, Cheng V, Samuel CS, Tang ML. The regulation of fibrosis in airway remodeling in asthma. Mol Cell Endocrinol. 2012; 351:167–175. [PubMed: 22266540]
47. Rydell-Tormanen K, Risse PA, Kanabar V, Bagchi R, Czubryt MP, Johnson JR. Smooth muscle in tissue remodeling and hyper-reactivity: airways and arteries. Pulm Pharmacol Ther. 2013; 26:13–23. [PubMed: 22561160]
48. Khan MA. Inflammation signals airway smooth muscle cell proliferation in asthma pathogenesis. Multidiscip Respir Med. 2013; 8:11. [PubMed: 23388501]
49. Vogel ER, VanOosten SK, Holman MA, Hohbein DD, Thompson MA, Vassallo R, Pandya HC, Prakash YS, Pabelick CM. Cigarette smoke enhances proliferation and extracellular matrix deposition by human fetal airway smooth muscle. Am J Physiol Lung Cell Mol Physiol. 2014; 307:L978–L986. [PubMed: 25344066]
50. Forteza RM, Casalino-Matsuda SM, Falcon NS, Valencia Gattas M, Monzon ME. Hyaluronan and layilin mediate loss of airway epithelial barrier function induced by cigarette smoke by decreasing E-cadherin. J Biol Chem. 2012; 287:42288–42298. [PubMed: 23048036]
51. Heijink IH, Brandenburg SM, Postma DS, van Oosterhout AJ. Cigarette smoke impairs airway epithelial barrier function and cell-cell contact recovery. Eur Respir J. 2012; 39:419–428. [PubMed: 21778164]
52. Holgate ST. Epithelium dysfunction in asthma. J Allergy Clin Immunol. 2007; 120:1233–1244. quiz 1245-1236. [PubMed: 18073119]
53. Rusznak C, Sapsford RJ, Devalia JL, Justin John R, Hewitt EL, Lamont AG, Wood AJ, Shah SS, Davies RJ, Lozewicz S. Cigarette smoke potentiates house dust mite allergen-induced increase in the permeability of human bronchial epithelial cells in vitro. Am J Respir Cell Mol Biol. 1999; 20:1238–1250. [PubMed: 10340943]
54. Shaykhiev R, Otaki F, Bonsu P, Dang DT, Teater M, Strulovici-Barel Y, Salit J, Harvey BG, Crystal RG. Cigarette smoking reprograms apical junctional complex molecular architecture in the human airway epithelium in vivo. Cellular and molecular life sciences : CMLS. 2011; 68:877–892. [PubMed: 20820852]
55. Fust A, Bates JH, Ludwig MS. Mechanical properties of mouse distal lung: in vivo versus in vitro comparison. Respir Physiol Neurobiol. 2004; 143:77–86. [PubMed: 15477174]
56. Sridhar S, Schembri F, Zeskind J, Shah V, Gustafson AM, Steiling K, Liu G, Dumas YM, Zhang X, Brody JS, Lenburg ME, Spira A. Smoking-induced gene expression changes in the bronchial airway are reflected in nasal and buccal epithelium. BMC Genomics. 2008; 9:259. [PubMed: 18513428]
57. Swindle EJ, Collins JE, Davies DE. Breakdown in epithelial barrier function in patients with asthma: identification of novel therapeutic approaches. J Allergy Clin Immunol. 2009; 124:23–34. quiz 35-26. [PubMed: 19560576]

58. Cadwell K, Liu JY, Brown SL, Miyoshi H, Loh J, Lennerz JK, Kishi C, Kc W, Carrero JA, Hunt S, Stone CD, Brunt EM, Xavier RJ, Sleckman BP, Li E, Mizushima N, Stappenbeck TS, Virgin HWt. A key role for autophagy and the autophagy gene Atg16l1 in mouse and human intestinal Paneth cells. Nature. 2008; 456:259–263. [PubMed: 18849966]
59. Prakash YS, Iyanoye A, Ay B, Mantilla CB, Pabelick CM. Neurotrophin effects on intracellular Ca2+ and force in airway smooth muscle. Am J Physiol Lung Cell Mol Physiol. 2006; 291:L447–L456. [PubMed: 16648236]
60. Prakash YS, Sathish V, Thompson MA, Pabelick CM, Sieck GC. Asthma and sarcoplasmic reticulum Ca2+ reuptake in airway smooth muscle. Am J Physiol Lung Cell Mol Physiol. 2009; 297:L794. [PubMed: 19783641]
61. Prakash YS, Thompson MA, Pabelick CM. Brain-derived neurotrophic factor in TNF-alpha modulation of Ca2+ in human airway smooth muscle. Am J Respir Cell Mol Biol. 2009; 41:603–611. [PubMed: 19213875]
62. Vassallo R, Tamada K, Lau JS, Kroening PR, Chen L. Cigarette smoke extract suppresses human dendritic cell function leading to preferential induction of Th-2 priming. J Immunol. 2005; 175:2684–2691. [PubMed: 16081845]
63. Blue ML, Janoff A. Possible mechanisms of emphysema in cigarette smokers. Release of elastase from human polymorphonuclear leukocytes by cigarette smoke condensate in vitro. Am Rev Respir Dis. 1978; 117:317–325. [PubMed: 637413]
64. Blanchet L, Buydens MC, Smeitink JA, Willems PH, Koopman WJ. Isolated mitochondrial complex I deficiency: explorative data analysis of patient cell parameters. Current pharmaceutical design. 2011; 17:4023–4033. [PubMed: 22188452]
65. Koopman WJ, Verkaart S, Visch HJ, van Emst-de Vries S, Nijtmans LG, Smeitink JA, Willems PH. Human NADH:ubiquinone oxidoreductase deficiency: radical changes in mitochondrial morphology? American journal of physiology. Cell physiology. 2007; 293:C22–C29. [PubMed: 17428841]
66. Dranka BP, Benavides GA, Diers AR, Giordano S, Zelickson BR, Reily C, Zou L, Chatham JC, Hill BG, Zhang J, Landar A, Darley-Usmar VM. Assessing bioenergetic function in response to oxidative stress by metabolic profiling. Free Radic Biol Med. 2011; 51:1621–1635. [PubMed: 21872656]
67. Zhou W, Choi M, Margineantu D, Margaretha L, Hesson J, Cavanaugh C, Blau CA, Horwitz MS, Hockenbery D, Ware C, Ruohola-Baker H. HIF1alpha induced switch from bivalent to exclusively glycolytic metabolism during ESC-to-EpiSC/hESC transition. EMBO J. 2012; 31:2103–2116. [PubMed: 22446391]
68. Ehrenberg B, Montana V, Wei MD, Wuskell JP, Loew LM. Membrane potential can be determined in individual cells from the nernstian distribution of cationic dyes. Biophysical journal. 1988; 53:785–794. [PubMed: 3390520]
69. Farkas DL, Wei MD, Febbroriello P, Carson JH, Loew LM. Simultaneous imaging of cell and mitochondrial membrane potentials. Biophysical journal. 1989; 56:1053–1069. [PubMed: 2611324]
70. Aravamudan B, Thompson M, Pabelick C, Prakash YS. Brain-derived neurotrophic factor induces proliferation of human airway smooth muscle cells. J Cell Mol Med. 2012; 16:812–823. [PubMed: 21651720]
71. Kroening PR, Barnes TW, Pease L, Limper A, Kita H, Vassallo R. Cigarette smoke-induced oxidative stress suppresses generation of dendritic cell IL-12 and IL-23 through ERK-dependent pathways. J Immunol. 2008; 181:1536–1547. [PubMed: 18606709]
72. Vassallo R, Kroening PR, Parambil J, Kita H. Nicotine and oxidative cigarette smoke constituents induce immune-modulatory and pro-inflammatory dendritic cell responses. Molecular immunology. 2008; 45:3321–3329. [PubMed: 18533267]
73. Aravamudan B, VanOosten SK, Meuchel LW, Vohra P, Thompson M, Sieck GC, Prakash YS, Pabelick CM. Caveolin-1 knockout mice exhibit airway hyperreactivity. Am J Physiol Lung Cell Mol Physiol. 2012; 303:L669–L681. [PubMed: 22923642]
74. Papkovsky DB, Hynes J, Will Y. Respirometric Screening Technology for ADME-Tox studies. Expert opinion on drug metabolism & toxicology. 2006; 2:313–323. [PubMed: 16866616]

75. Sakamuru S, Li X, Attene-Ramos MS, Huang R, Lu J, Shou L, Shen M, Tice RR, Austin CP, Xia M. Application of a homogenous membrane potential assay to assess mitochondrial function. Physiol Genomics. 2012; 44:495–503. [PubMed: 22433785]
76. Legros F, Lombes A, Frachon P, Rojo M. Mitochondrial fusion in human cells is efficient, requires the inner membrane potential, and is mediated by mitofusins. Mol Biol Cell. 2002; 13:4343–4354. [PubMed: 12475957]
77. Mattenberger Y, James DI, Martinou JC. Fusion of mitochondria in mammalian cells is dependent on the mitochondrial inner membrane potential and independent of microtubules or actin. FEBS Lett. 2003; 538:53–59. [PubMed: 12633852]
78. Archer SL, Marsboom G, Kim GH, Zhang HJ, Toth PT, Svensson EC, Dyck JR, Gomberg-Maitland M, Thebaud B, Husain AN, Cipriani N, Rehman J. Epigenetic attenuation of mitochondrial superoxide dismutase 2 in pulmonary arterial hypertension: a basis for excessive cell proliferation and a new therapeutic target. Circulation. 2010; 121:2661–2671. [PubMed: 20529999]
79. Chalmers S, Saunter C, Wilson C, Coats P, Girkin JM, McCarron JG. Mitochondrial motility and vascular smooth muscle proliferation. Arteriosclerosis, thrombosis, and vascular biology. 2012; 32:3000–3011.
80. Chen KH, Guo X, Ma D, Guo Y, Li Q, Yang D, Li P, Qiu X, Wen S, Xiao RP, Tang J. Dysregulation of HSG triggers vascular proliferative disorders. Nat Cell Biol. 2004; 6:872–883. [PubMed: 15322553]
81. Guo X, Chen KH, Guo Y, Liao H, Tang J, Xiao RP. Mitofusin 2 triggers vascular smooth muscle cell apoptosis via mitochondrial death pathway. Circ Res. 2007; 101:1113–1122. [PubMed: 17901359]
82. Nagaraj R, Gururaja-Rao S, Jones KT, Slattery M, Negre N, Braas D, Christofk H, White KP, Mann R, Banerjee U. Control of mitochondrial structure and function by the Yorkie/YAP oncogenic pathway. Genes & development. 2012; 26:2027–2037. [PubMed: 22925885]
83. Rehman J, Zhang HJ, Toth PT, Zhang Y, Marsboom G, Hong Z, Salgia R, Husain AN, Wietholt C, Archer SL. Inhibition of mitochondrial fission prevents cell cycle progression in lung cancer. FASEB J. 2012; 26:2175–2186. [PubMed: 22321727]
84. Agarwal AR, Yin F, Cadenas E. Short-term cigarette smoke exposure leads to metabolic alterations in lung alveolar cells. Am J Respir Cell Mol Biol. 2014; 51:284–293. [PubMed: 24625219]
85. Agarwal AR, Zhao L, Sancheti H, Sundar IK, Rahman I, Cadenas E. Short-term cigarette smoke exposure induces reversible changes in energy metabolism and cellular redox status independent of inflammatory responses in mouse lungs. Am J Physiol Lung Cell Mol Physiol. 2012; 303:L889–L898. [PubMed: 23064950]
86. Kim MS, Huang Y, Lee J, Zhong X, Jiang WW, Ratovitski EA, Sidransky D. Cellular transformation by cigarette smoke extract involves alteration of glycolysis and mitochondrial function in esophageal epithelial cells. International journal of cancer. Journal international du cancer. 2010; 127:269–281. [PubMed: 19937795]
87. Guillery O, Malka F, Frachon P, Milea D, Rojo M, Lombes A. Modulation of mitochondrial morphology by bioenergetics defects in primary human fibroblasts. Neuromuscul Disord. 2008; 18:319–330. [PubMed: 18395446]
88. Benard G, Bellance N, James D, Parrone P, Fernandez H, Letellier T, Rossignol R. Mitochondrial bioenergetics and structural network organization. J Cell Sci. 2007; 120:838–848. [PubMed: 17298981]
89. Hill BG, Higdon AN, Dranka BP, Darley-Usmar VM. Regulation of vascular smooth muscle cell bioenergetic function by protein glutathiolation. Biochim Biophys Acta. 2010; 1797:285–295. [PubMed: 19925774]
90. Adam-Vizi V. Production of reactive oxygen species in brain mitochondria: contribution by electron transport chain and non-electron transport chain sources. Antioxid Redox Signal. 2005; 7:1140–1149. [PubMed: 16115017]
91. Puente-Maestu L, Perez-Parra J, Godoy R, Moreno N, Tejedor A, Gonzalez-Aragoneses F, Bravo JL, Alvarez FV, Camano S, Agusti A. Abnormal mitochondrial function in locomotor and respiratory muscles of COPD patients. Eur Respir J. 2009; 33:1045–1052. [PubMed: 19129279]

92. Boldogh I, Bacsi A, Choudhury BK, Dharajiya N, Alam R, Hazra TK, Mitra S, Goldblum RM, Sur S. ROS generated by pollen NADPH oxidase provide a signal that augments antigen-induced allergic airway inflammation. J Clin Invest. 2005; 115:2169–2179. [PubMed: 16075057]

93. Hwang MS, Rohlena J, Dong LF, Neuzil J, Grimm S. Powerhouse down: Complex II dissociation in the respiratory chain. Mitochondrion. 2014; 19(Pt A):20–28. [PubMed: 24933571]

94. Miettinen M, Killian JK, Wang ZF, Lasota J, Lau C, Jones L, Walker R, Pineda M, Zhu YJ, Kim SY, Helman L, Meltzer P. Immunohistochemical loss of succinate dehydrogenase subunit A (SDHA) in gastrointestinal stromal tumors (GISTs) signals SDHA germline mutation. Am J Surg Pathol. 2013; 37:234–240. [PubMed: 23282968]

95. Kim YH, Jung WH, Koo JS. Expression of metabolism-related proteins in invasive lobular carcinoma: comparison to invasive ductal carcinoma. Tumour Biol. 2014; 35:10381–10393. [PubMed: 25053597]

96. Gao YD, Zou JJ, Zheng JW, Shang M, Chen X, Geng S, Yang J. Promoting effects of IL-13 on Ca2+ release and store-operated Ca2+ entry in airway smooth muscle cells. Pulm Pharmacol Ther. 2010; 23:182–189. [PubMed: 20045483]

97. Hill BG, Dranka BP, Zou L, Chatham JC, Darley-Usmar VM. Importance of the bioenergetic reserve capacity in response to cardiomyocyte stress induced by 4-hydroxynonenal. Biochem J. 2009; 424:99–107. [PubMed: 19740075]

98. Nicholls DG. Spare respiratory capacity, oxidative stress and excitotoxicity. Biochemical Society transactions. 2009; 37:1385–1388. [PubMed: 19909281]

99. Nicholls DG, Darley-Usmar VM, Wu M, Jensen PB, Rogers GW, Ferrick DA. Bioenergetic profile experiment using C2C12 myoblast cells. J Vis Exp. 2010

100. Yadava N, Nicholls DG. Spare respiratory capacity rather than oxidative stress regulates glutamate excitotoxicity after partial respiratory inhibition of mitochondrial complex I with rotenone. J Neurosci. 2007; 27:7310–7317. [PubMed: 17611283]

101. van der Windt GJ, Everts B, Chang CH, Curtis JD, Freitas TC, Amiel E, Pearce EJ, Pearce EL. Mitochondrial respiratory capacity is a critical regulator of CD8+ T cell memory development. Immunity. 2012; 36:68–78. [PubMed: 22206904]

102. Chacko BK, Kramer PA, Ravi S, Benavides GA, Mitchell T, Dranka BP, Ferrick D, Singal AK, Ballinger SW, Bailey SM, Hardy RW, Zhang J, Zhi D, Darley-Usmar VM. The Bioenergetic Health Index: a new concept in mitochondrial translational research. Clinical science. 2014; 127:367–373. [PubMed: 24895057]

103. Warburg O. On respiratory impairment in cancer cells. Science. 1956; 124:269–270. [PubMed: 13351639]

104. Archer SL, Gomberg-Maitland M, Maitland ML, Rich S, Garcia JG, Weir EK. Mitochondrial metabolism, redox signaling, and fusion: a mitochondria-ROS-HIF-1alpha-Kv1.5 O2-sensing pathway at the intersection of pulmonary hypertension and cancer. Am J Physiol Heart Circ Physiol. 2008; 294:H570–H578. [PubMed: 18083891]

105. Rehman J, Archer SL. A proposed mitochondrial-metabolic mechanism for initiation and maintenance of pulmonary arterial hypertension in fawn-hooded rats: the Warburg model of pulmonary arterial hypertension. Advances in experimental medicine and biology. 2010; 661:171–185. [PubMed: 20204730]

106. Fu QF, Liu Y, Fan Y, Hua SN, Qu HY, Dong SW, Li RL, Zhao MY, Zhen Y, Yu XL, Chen YY, Luo RC, Li R, Li LB, Deng XJ, Fang WY, Liu Z, Song X. Alpha-enolase promotes cell glycolysis, growth, migration, and invasion in non-small cell lung cancer through FAK-mediated PI3K/AKT pathway. J Hematol Oncol. 2015; 8:22. [PubMed: 25887760]

107. Principe M, Ceruti P, Shih NY, Chattaragada MS, Rolla S, Conti L, Bestagno M, Zentilin L, Yang SH, Migliorini P, Cappello P, Burrone O, Novelli F. Targeting of surface alpha-enolase inhibits the invasiveness of pancreatic cancer cells. Oncotarget. 2015; 6:11098–11113. [PubMed: 25860938]

108. Royds JA, Timperley WR, Taylor CB. Levels of enolase and other enzymes in the cerebrospinal fluid as indices of pathological change. J Neurol Neurosurg Psychiatry. 1981; 44:1129–1135. [PubMed: 7334408]

109. Zhu X, Miao X, Wu Y, Li C, Guo Y, Liu Y, Chen Y, Lu X, Wang Y, He S. ENO1 promotes tumor proliferation and cell adhesion mediated drug resistance (CAM-DR) in Non-Hodgkin's Lymphomas. Exp Cell Res. 2015; 335:216–223. [PubMed: 26024773]
110. Liu X, Yang Z, Chen Z, Chen R, Zhao D, Zhou Y, Qiao L. Effects of the suppression of lactate dehydrogenase A on the growth and invasion of human gastric cancer cells. Oncol Rep. 2015; 33:157–162. [PubMed: 25394466]
111. Qiu H, Jackson AL, Kilgore JE, Zhong Y, Chan LL, Gehrig PA, Zhou C, Bae-Jump VL. JQ1 suppresses tumor growth through downregulating LDHA in ovarian cancer. Oncotarget. 2015; 6:6915–6930. [PubMed: 25762632]
112. Xian ZY, Liu JM, Chen QK, Chen HZ, Ye CJ, Xue J, Yang HQ, Li JL, Liu XF, Kuang SJ. Inhibition of LDHA suppresses tumor progression in prostate cancer. Tumour Biol. 2015; 36:8093–8100. [PubMed: 25983002]
113. Zhou X, Chen R, Xie W, Ni Y, Liu J, Huang G. Relationship between 18F-FDG accumulation and lactate dehydrogenase A expression in lung adenocarcinomas. J Nucl Med. 2014; 55:1766–1771. [PubMed: 25342384]
114. Mohammad MK, Avila D, Zhang J, Barve S, Arteel G, McClain C, Joshi-Barve S. Acrolein cytotoxicity in hepatocytes involves endoplasmic reticulum stress, mitochondrial dysfunction and oxidative stress. Toxicology and applied pharmacology. 2012; 265:73–82. [PubMed: 23026831]
115. Thatcher MO, Tippetts TS, Nelson MB, Swensen AC, Winden DR, Hansen ME, Anderson MC, Johnson IE, Porter JP, Reynolds PR, Bikman BT. Ceramides mediate cigarette smoke-induced metabolic disruption in mice. American journal of physiology. Endocrinology and metabolism. 2014; 307:E919–E927. [PubMed: 25269485]
116. Du H, Sun J, Chen Z, Nie J, Tong J, Li J. Cigarette smoke-induced failure of apoptosis resulting in enhanced neoplastic transformation in human bronchial epithelial cells. Journal of toxicology and environmental health. Part A. 2012; 75:707–720. [PubMed: 22757675]
117. Ferecatu I, Borot MC, Bossard C, Leroux M, Boggetto N, Marano F, Baeza-Squiban A, Andreau K. Polycyclic aromatic hydrocarbon components contribute to the mitochondria-antiapoptotic effect of fine particulate matter on human bronchial epithelial cells via the aryl hydrocarbon receptor. Particle and fibre toxicology. 2010; 7:18. [PubMed: 20663163]
118. Salem AF, Al-Zoubi MS, Whitaker-Menezes D, Martinez-Outschoorn UE, Lamb R, Hulit J, Howell A, Gandara R, Sartini M, Galbiati F, Bevilacqua G, Sotgia F, Lisanti MP. Cigarette smoke metabolically promotes cancer, via autophagy and premature aging in the host stromal microenvironment. Cell Cycle. 2013; 12:818–825. [PubMed: 23388463]
119. Baglole CJ, Bushinsky SM, Garcia TM, Kode A, Rahman I, Sime PJ, Phipps RP. Differential induction of apoptosis by cigarette smoke extract in primary human lung fibroblast strains: implications for emphysema. Am J Physiol Lung Cell Mol Physiol. 2006; 291:L19–L29. [PubMed: 16443644]
120. Du CL, Xu YJ, Liu XS, Xie JG, Xie M, Zhang ZX, Zhang J, Qiao LF. Up-regulation of cyclin D1 expression in asthma serum-sensitized human airway smooth muscle promotes proliferation via protein kinase C alpha. Exp Lung Res. 2010; 36:201–210. [PubMed: 20426528]
121. Estaquier J, Arnoult D. Inhibiting Drp1-mediated mitochondrial fission selectively prevents the release of cytochrome c during apoptosis. Cell Death Differ. 2007; 14:1086–1094. [PubMed: 17332775]
122. Guo C, Hildick KL, Luo J, Dearden L, Wilkinson KA, Henley JM. SENP3-mediated deSUMOylation of dynamin-related protein 1 promotes cell death following ischaemia. EMBO J. 2013; 32:1514–1528. [PubMed: 23524851]
123. Inoue-Yamauchi A, Oda H. Depletion of mitochondrial fission factor DRP1 causes increased apoptosis in human colon cancer cells. Biochem Biophys Res Commun. 2012; 421:81–85. [PubMed: 22487795]
124. Marsboom G, Toth PT, Ryan JJ, Hong Z, Wu X, Fang YH, Thenappan T, Piao L, Zhang HJ, Pogoriler J, Chen Y, Morrow E, Weir EK, Rehman J, Archer SL. Dynamin-related protein 1-mediated mitochondrial mitotic fission permits hyperproliferation of vascular smooth muscle cells and offers a novel therapeutic target in pulmonary hypertension. Circ Res. 2012; 110:1484–1497. [PubMed: 22511751]

125. Cecconi F, Levine B. The role of autophagy in mammalian development: cell makeover rather than cell death. Dev Cell. 2008; 15:344–357. [PubMed: 18804433]

126. Glick D, Barth S, Macleod KF. Autophagy: cellular and molecular mechanisms. The Journal of pathology. 2010; 221:3–12. [PubMed: 20225336]

127. Goldsmith J, Levine B, Debnath J. Autophagy and cancer metabolism. Methods in enzymology. 2014; 542:25–57. [PubMed: 24862259]

128. Poillet-Perez L, Despouy G, Delage-Mourroux R, Boyer-Guittaut M. Interplay between ROS and autophagy in cancer cells, from tumor initiation to cancer therapy. Redox biology. 2015; 4:184–192. [PubMed: 25590798]

129. Ryter SW, Choi AM. Autophagy in lung disease pathogenesis and therapeutics. Redox biology. 2015; 4:215–225. [PubMed: 25617802]

130. Mizumura K, Cloonan SM, Nakahira K, Bhashyam AR, Cervo M, Kitada T, Glass K, Owen CA, Mahmood A, Washko GR, Hashimoto S, Ryter SW, Choi AM. Mitophagy-dependent necroptosis contributes to the pathogenesis of COPD. J Clin Invest. 2014; 124:3987–4003. [PubMed: 25083992]

131. Ryter SW, Nakahira K, Haspel JA, Choi AM. Autophagy in pulmonary diseases. Annu Rev Physiol. 2012; 74:377–401. [PubMed: 22035347]

132. Egan DF, Shackelford DB, Mihaylova MM, Gelino S, Kohnz RA, Mair W, Vasquez DS, Joshi A, Gwinn DM, Taylor R, Asara JM, Fitzpatrick J, Dillin A, Viollet B, Kundu M, Hansen M, Shaw RJ. Phosphorylation of ULK1 (hATG1) by AMP-activated protein kinase connects energy sensing to mitophagy. Science. 2011; 331:456–461. [PubMed: 21205641]

133. Youle RJ, Narendra DP. Mechanisms of mitophagy. Nat Rev Mol Cell Biol. 2011; 12:9–14. [PubMed: 21179058]

134. Aravamudan B, Thompson MA, Pabelick CM, Prakash YS. Mitochondria in lung diseases. Expert review of respiratory medicine. 2013; 7:631–646. [PubMed: 23978003]

135. Araya J, Kojima J, Takasaka N, Ito S, Fujii S, Hara H, Yanagisawa H, Kobayashi K, Tsurushige C, Kawaishi M, Kamiya N, Hirano J, Odaka M, Morikawa T, Nishimura SL, Kawabata Y, Hano H, Nakayama K, Kuwano K. Insufficient autophagy in idiopathic pulmonary fibrosis. Am J Physiol Lung Cell Mol Physiol. 2013; 304:L56–L69. [PubMed: 23087019]

136. Green DR, Galluzzi L, Kroemer G. Mitochondria and the autophagy-inflammation-cell death axis in organismal aging. Science. 2011; 333:1109–1112. [PubMed: 21868666]

137. Mizushima N, Levine B, Cuervo AM, Klionsky DJ. Autophagy fights disease through cellular self-digestion. Nature. 2008; 451:1069–1075. [PubMed: 18305538]

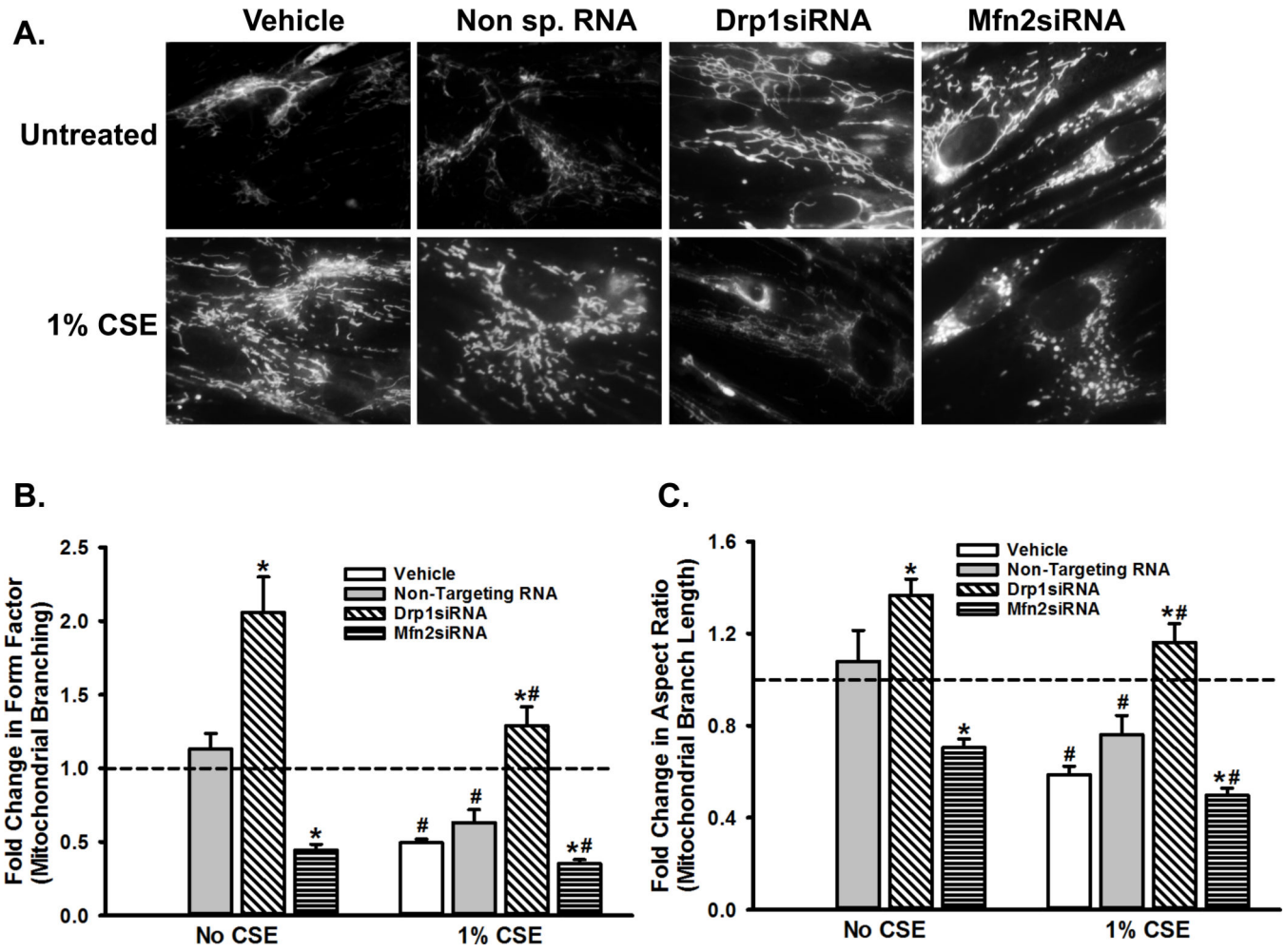

Figure 1. Mitochondrial morphology is dynamically regulated by chronic exposure of ASM cells to CS or by altering the expression of proteins involved in fission and fusion

ASM cells were transfected with siRNA against mitochondrial fission protein Drp1 or the fusion protein Mfn2, and were either exposed to medium or to 1% CSE for 48h. Mitochondria were marked by loading the cells with 400nM MitoTracker Green, and were imaged. 'Vehicle' refers to 'No Transfection' control where the transfection reagent Lipofectamine, with no DNA or RNA, was added to the cells. A non-specific siRNA was used to control for siRNA specificity. A) Representative images depicting the normal, fragmented or hyperfused morphology of the mitochondrial tracks in an ASM cell. B–C) Quantification of mitochondrial morphology, as assessed by Form Factor that measures mitochondrial branching (B), and Aspect Ratio that measures the length of the branches (C). Both Form Factor and Aspect Ratio are indictors of the complexity of mitochondrial network in a cell.

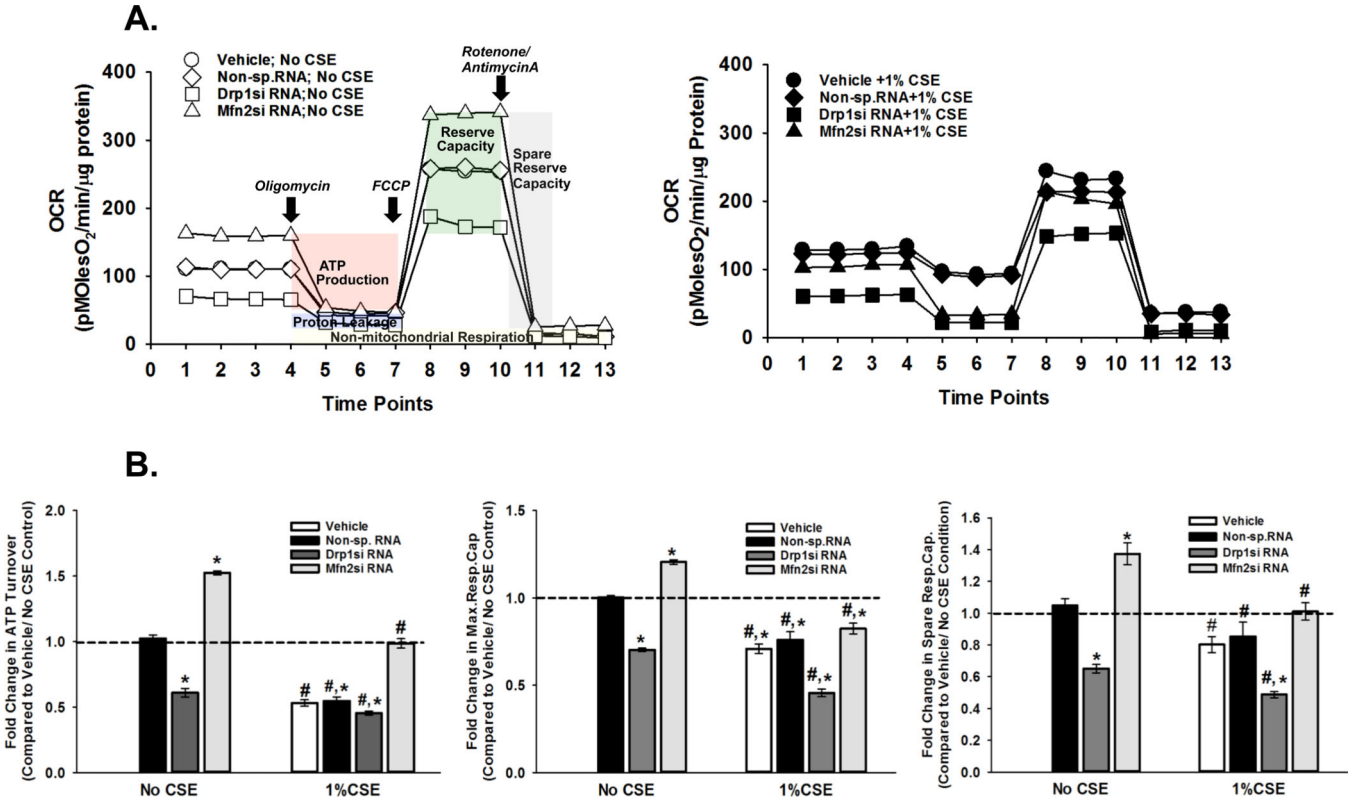

Figure 2. Energy metabolism is defective in CS-exposed ASM cells

ASM cells, transfected with siRNA against mitochondrial fission protein Drp1 or the fusion protein Mfn2, were either exposed to medium or 1% CSE for 24h before OCR (Oxygen consumption rate) was measured on an XF^{e}24 Extracellular Flux Analyzer. 'Vehicle' refers to 'No Transfection' control where the transfection reagent Lipofectamine, with no DNA or RNA, was added to the cells. A non-specific siRNA was used to control for siRNA specificity. **A.** Representative graphs depicting the OCR trends when the cells were unexposed (left) or exposed to 1% CSE (right). CS clearly reduces ATP production and Spare Reserve Capacity. **B.** Quantification of mitochondrial bioenergetics in terms of ATP production, Maximum Respiratory Capacity and Spare Respiratory Capacity. All three parameters are lowered by CS. (N=4; * indicates significant difference from 'Vehicle Only' control; # indicates significant difference between Unexposed and CS-exposed systems; $P<0.05$).

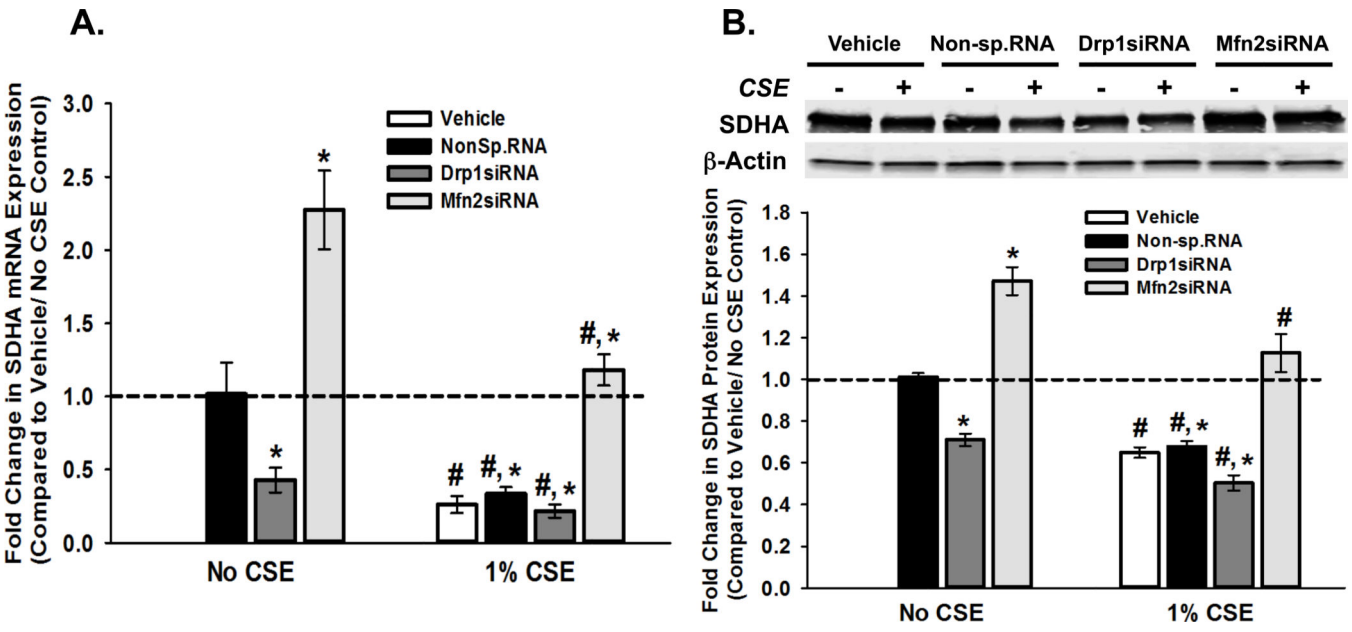

Figure 3. CS-induced fission-fusion imbalance regulates the expression of genes involved in mitochondrial energy metabolism in ASM cells

A–B. ASM cells, transfected with siRNA against mitochondrial fission protein Drp1 or the fusion protein Mfn2, were either exposed to medium or 1% CSE for 48h before total RNA or total protein was isolated. 'Vehicle' refers to 'No Transfection' control where the transfection reagent Lipofectamine, with no DNA or RNA, was added to the cells. A non-specific siRNA was used to control for siRNA specificity. **A.** Total RNA was reverse transcribed and the cDNA was used in Q-PCR to measure the expression of SDHA enzyme, a vital component of ETC (See Table 3 for another ETC marker ATP5A). Inhibition of fission (Drp1siRNA) lessens SDHA mRNA expression, while Mfn2siRNA augments it. Exposure to CS reduces SDHA expression in all four transfection systems. (N=4; * indicates significant difference from 'Vehicle Only' control; # indicates significant difference between Unexposed and CS-exposed systems; $P<0.05$). **B.** Expression of SDHA protein shows a trend similar to that of its mRNA. A representative gel is presented on top, with β-Actin as the loading control. The graph below depicts the quantification of protein expression from data collected from 4 different ASM populations. See Table 4 for another ETC protein ATP5A. (N=4; * indicates significant difference from 'Vehicle Only' control; # indicates significant difference between Unexposed and CS-exposed systems; $P<0.05$).

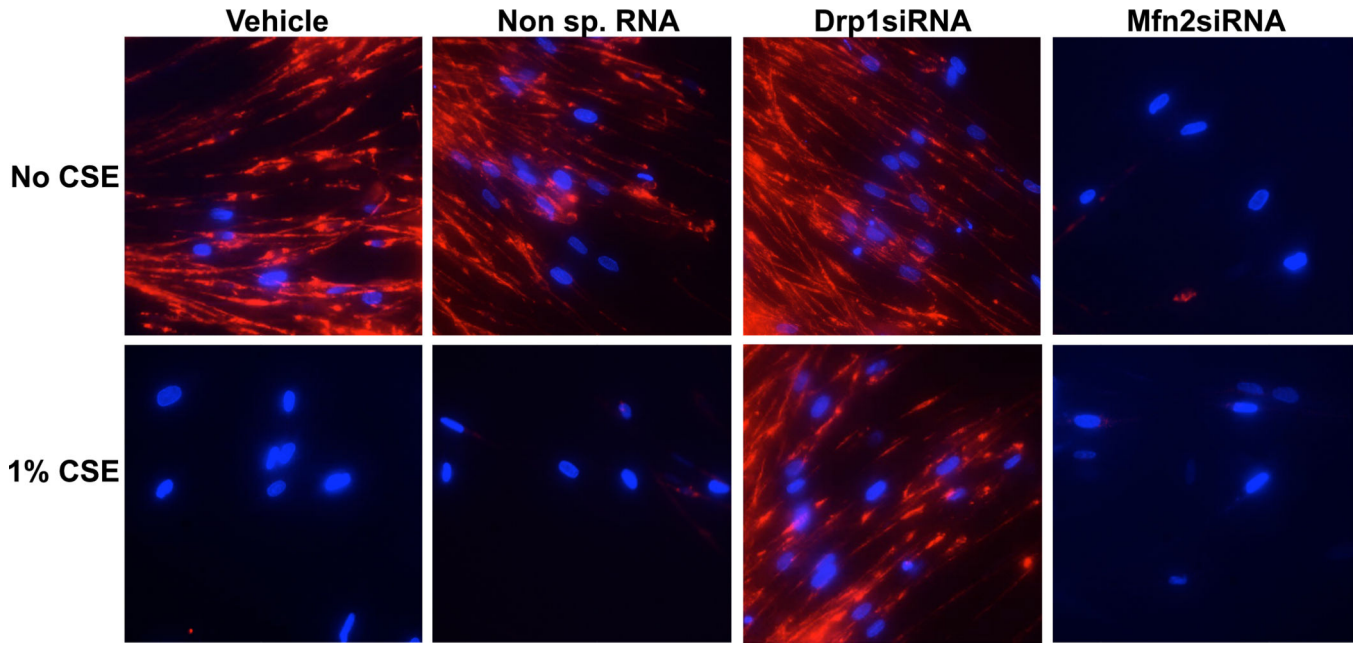

Figure 4. CS-regulation of mitochondrial membrane potential

ASM cells, transfected with siRNA against mitochondrial fission protein Drp1 or the fusion protein Mfn2, were either exposed to medium or 1% CSE for 48h before mitochondrial membrane integrity was visualized using 50 nM TMRE (Tetramethyl rhodamine ethyl ester; red). CSE and Mfn2siRNA, both of which instigate mitochondrial fragmentation, clearly cause a collapse in MMP. Cell nuclei are marked with DAPI (Blue). 'Vehicle' refers to 'No Transfection' control where the transfection reagent Lipofectamine was added to the cells in the absence of DNA or RNA. A non-specific siRNA was used to control for siRNA specificity.

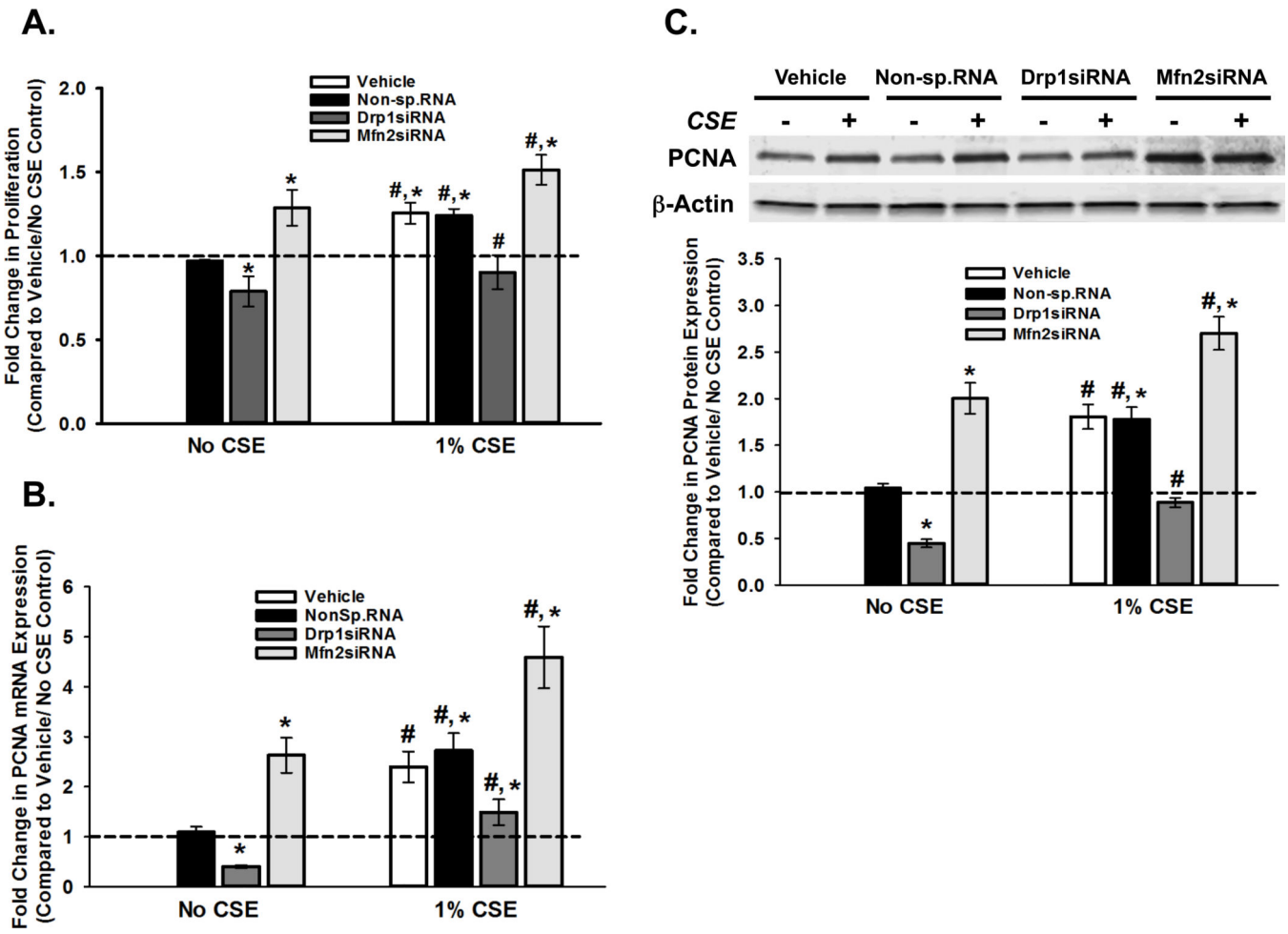

Figure 5. CS-regulation of mitochondrial morphology impacts ASM proliferation

ASM cells, transfected with siRNA against mitochondrial fission protein Drp1 or the fusion protein Mfn2, were either exposed to medium or 1% CSE for 48h before cell proliferation was assayed. 'Vehicle' refers to 'No Transfection' control where the transfection reagent Lipofectamine was added to the cells in the absence of DNA or RNA. A non-specific siRNA was used to control for siRNA specificity. **A.** Cell proliferation was measured using the CyQuant NF fluorescence dye system on a Flex Station3 microplate reader. Results indicate Drp1 to be pro-proliferative as inhibition via siRNA decreases proliferation; Conversely, Mfn2 is anti-proliferataive as siRNA treatment increases ASM cell proliferation. CS treatment increases proliferation in all systems. (N=4; * indicates significant difference from 'Vehicle Only' control; # indicates significant difference between unexposed and CS-exposed systems; $P<0.05$) **B–C.** ASM cells, transfected with siRNA against mitochondrial fission protein Drp1 or the fusion protein Mfn2, were either exposed to medium or 1% CSE for 48h before total RNA or total protein was isolated. **B.** Total RNA was reverse transcribed and the cDNA was used in Q-PCR to measure the expression of PCNA, a gene product that marks the onset of cell proliferation (See Table 3 for proliferation markers Bcl2 and Cyclin D). Expression of PCNA mRNA is downregulated when fission is inhibited (Drp1siRNA), and is upregulated when fusion is blocked (Mfn2siRNA). Exposure to CS elevates PCNA

expression in all four transfection systems. (N=4; * indicates significant difference from 'Vehicle Only' control; # indicates significant difference between unexposed and CS-exposed systems; P<0.05). **C.** Expression of PCNA protein shows a trend similar to that of its mRNA. A representative gel is presented with β-Actin as the loading control. The graph depicts the quantification of protein expression from data collected from 4 different ASM populations. See Table 4 for other proliferation proteins Cyclin D1 and Bcl2. (N=4; * indicates significant difference from 'Vehicle Only' control; # indicates significant difference between unexposed and CS-exposed systems; P<0.05).

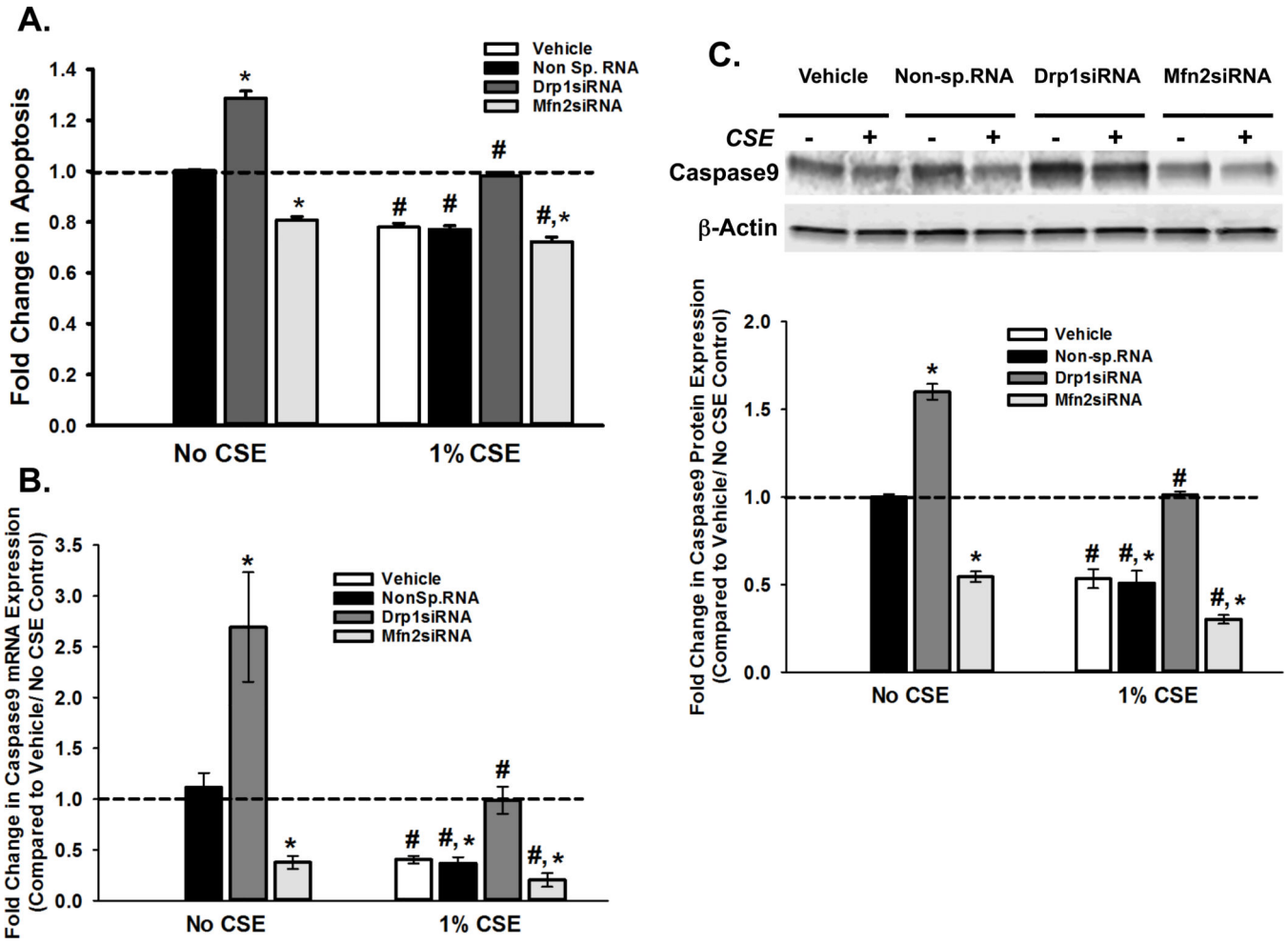

Figure 6. CS-regulation of mitochondrial morphology impacts ASM apoptosis

ASM cells, transfected with siRNA against mitochondrial fission protein Drp1 or the fusion protein Mfn2, were either exposed to medium or 1% CSE for 48h before apoptosis was assayed. 'Vehicle' refers to 'No Transfection' control where the transfection reagent Lipofectamine was added to the cells in the absence of DNA or RNA. A non-specific siRNA was used to control for siRNA specificity. **A.** Apoptotic cell death was measured using the Multiparameter Apoptosis Kit, which integrates fluorescence readings from MMP marker TMRE and cell number and nuclear morphology marker Hoechst dye with those of apoptosis marker Annexin V. Drp1 seems to be anti-apoptotic, as its inhibition via siRNA increases cell death; Mfn2, on the other hand promotes apoptosis. CS treatment increases proliferation in all systems. (N=4; * indicates significant difference from 'Vehicle Only' control; # indicates significant difference between unexposed and CS-exposed systems; $P<0.05$). **B–C.** ASM cells, transfected with siRNA against mitochondrial fission protein Drp1 or the fusion protein Mfn2, were either exposed to medium or 1% CSE for 48h before total RNA or total protein was isolated. 'Vehicle' refers to 'No Transfection' control where the transfection reagent Lipofectamine was added to the cells in the absence of DNA or RNA. A non-specific siRNA was used to control for siRNA specificity. **A.** Total RNA was reverse transcribed and the cDNA was used in Q-PCR to measure the expression of

Caspase9, a marker for apoptosis (See Table 3 for another marker Cytochrome C). Expression of Caspase9 mRNA increases when fission is inhibited (Drp1siRNA), and is lowered when fusion is blocked (Mfn2siRNA). Exposure to CS reduces Caspase9 expression in all four transfection systems. (N=4; * indicates significant difference from 'Vehicle Only' control; # indicates significant difference between unexposed and CS-exposed systems; $P<0.05$). **B.** Expression of Caspase9 protein shows a trend similar to that of its mRNA. A representative gel is presented with β-Actin as the loading control. The graph depicts the quantification of protein expression from data collected from 4 different ASM populations. See Table 4 for another apoptosis protein Cytochrome C. (N=4; * indicates significant difference from 'Vehicle Only' control; # indicates significant difference between unexposed and CS-exposed systems; $P<0.05$).

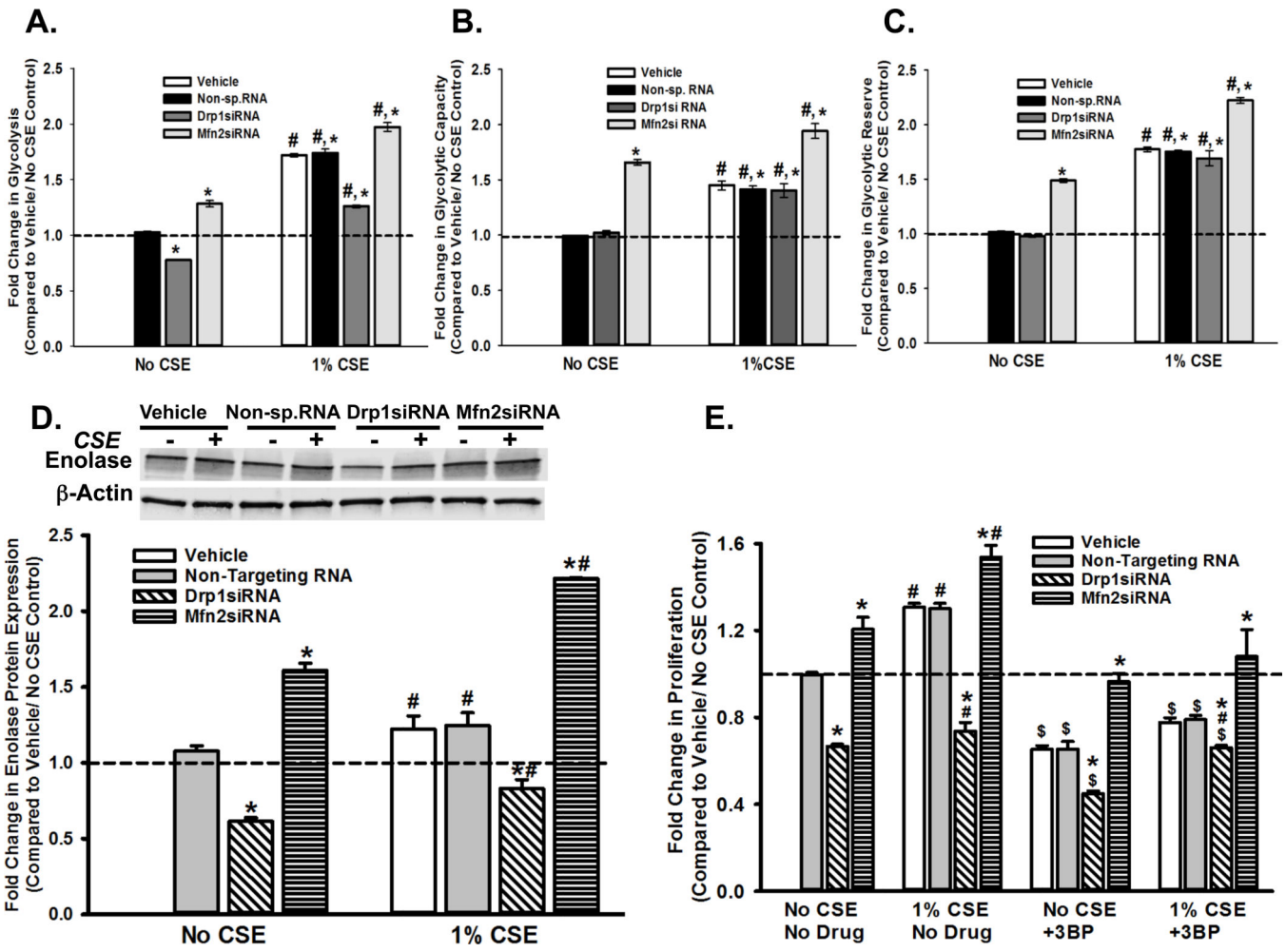

Figure 7. CS exposure and perturbation of mitochondrial fission-fusion balance drive ASM cells towards glycolysis for ATP production

A–C. ASM cells, transfected with siRNA against mitochondrial fission protein Drp1 or the fusion protein Mfn2, were either exposed to medium or 1% CSE for 24h before ECAR (Extracellular acidification rate), an indicator of glycolysis, was measured on an XF^{e}24 Extracellular Flux Analyzer. 'Vehicle' refers to 'No Transfection' control where the transfection reagent Lipofectamine, with no DNA or RNA, was added to the cells. A non-specific siRNA was used to control for siRNA specificity. An increase was observed in all three aspects of ECAR: the rate of glycolysis (**A**) glycolytic capacity **(B)** and glycolytic reserve **(C)**, following CS exposure. (N=4; * indicates significant difference from 'Vehicle Only' control; # indicates significant difference between unexposed and CS-exposed systems; $P<0.05$) **D.** Total protein was isolated from untransfected, and Drp1- or Mfn2siRNA-transfected ASM cells and subjected to immunoblotting to analyze expression of glycolysis marker Enolase. (See Table 4 for another glycolysis marker LDHA). Inhibition of fission (Drp1siRNA) lessens Enolase expression, while Mfn2siRNA augments it. A representative gel is presented with β-Actin as the loading control. The graph depicts the quantification of protein expression from data collected from 4 different ASM populations. Exposure to CS elevates Enolase expression in all four transfection systems. (N=4; *

indicates significant difference from ‘Vehicle Only’ control; # indicates significant difference between unexposed and CS-exposed systems; P<0.05). **E.** Untransfected, and Drp1- or Mfn2siRNA-transfected ASM cells were treated with 100 μM 3-BP, an inhibitor of an early stage glycolysis enzyme hexokinase, before CS exposure. Cell proliferation was measured using the CyQuant NF fluorescence dye system on a Flex Station3 microplate reader. Results indicate inhibition of proliferation by 3-BP. CS treatment partially reverses 3-BP effects. (N=4; * indicates significant difference from ‘Vehicle Only’ control; # indicates significant difference between unexposed and CS-exposed systems; P<0.05)

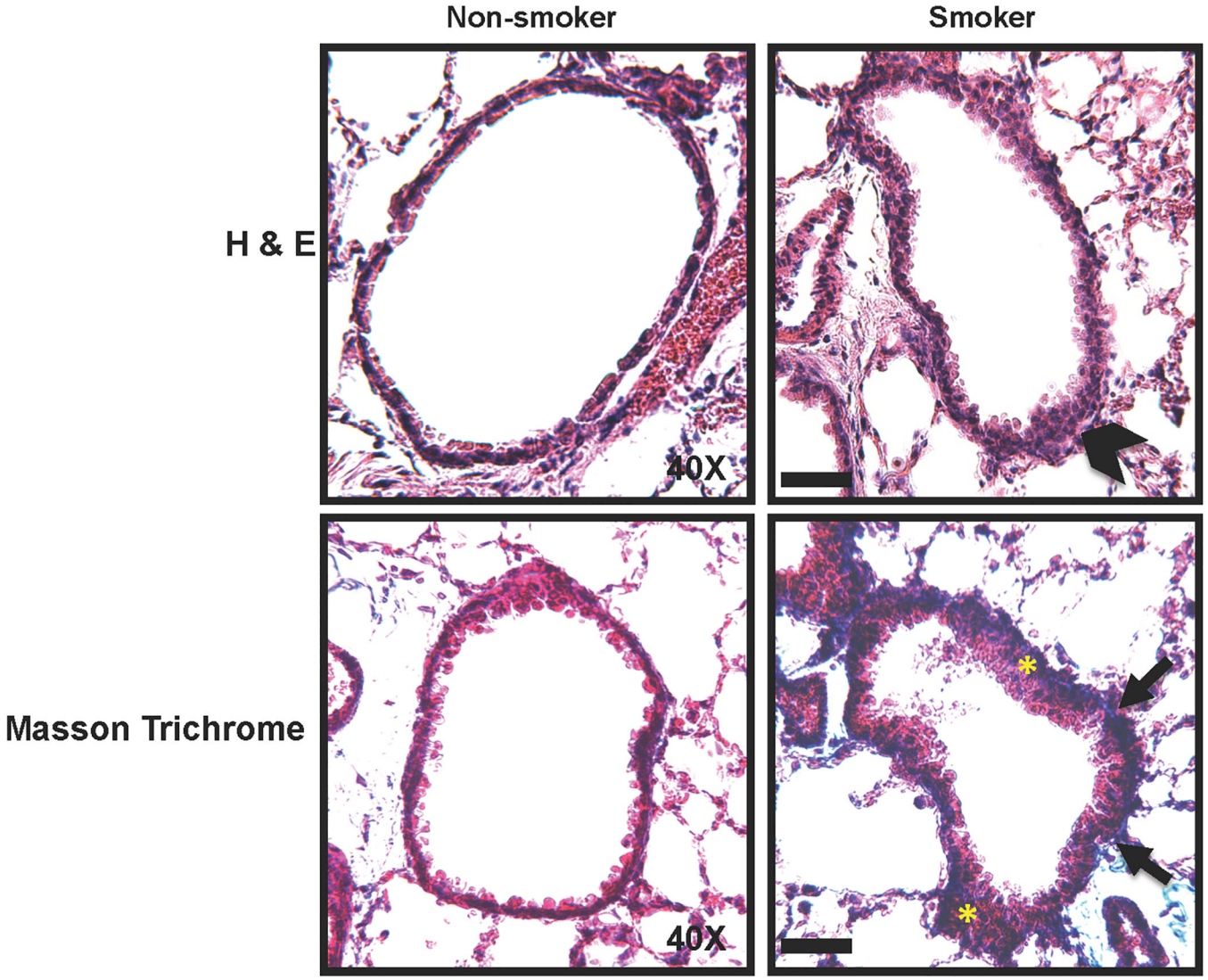

Figure 8. Chronic exposure to CS causes airway thickening and remodeling

A mouse model of chronic CS exposure was developed and lungs processed for histology (see Methods for details). Hematoxylin and eosin (H&E) and Masson Trichrome staining protocols were performed on 5μm lung sections. Increased thickening of the airway (arrowhead) enhanced cell proliferation (yellow asterisks) and pronounced collagen infiltration (blue fibrous staining denoted by arrows) are evident in the lung sections from CS-exposed mice. Scale bar = 50μm.

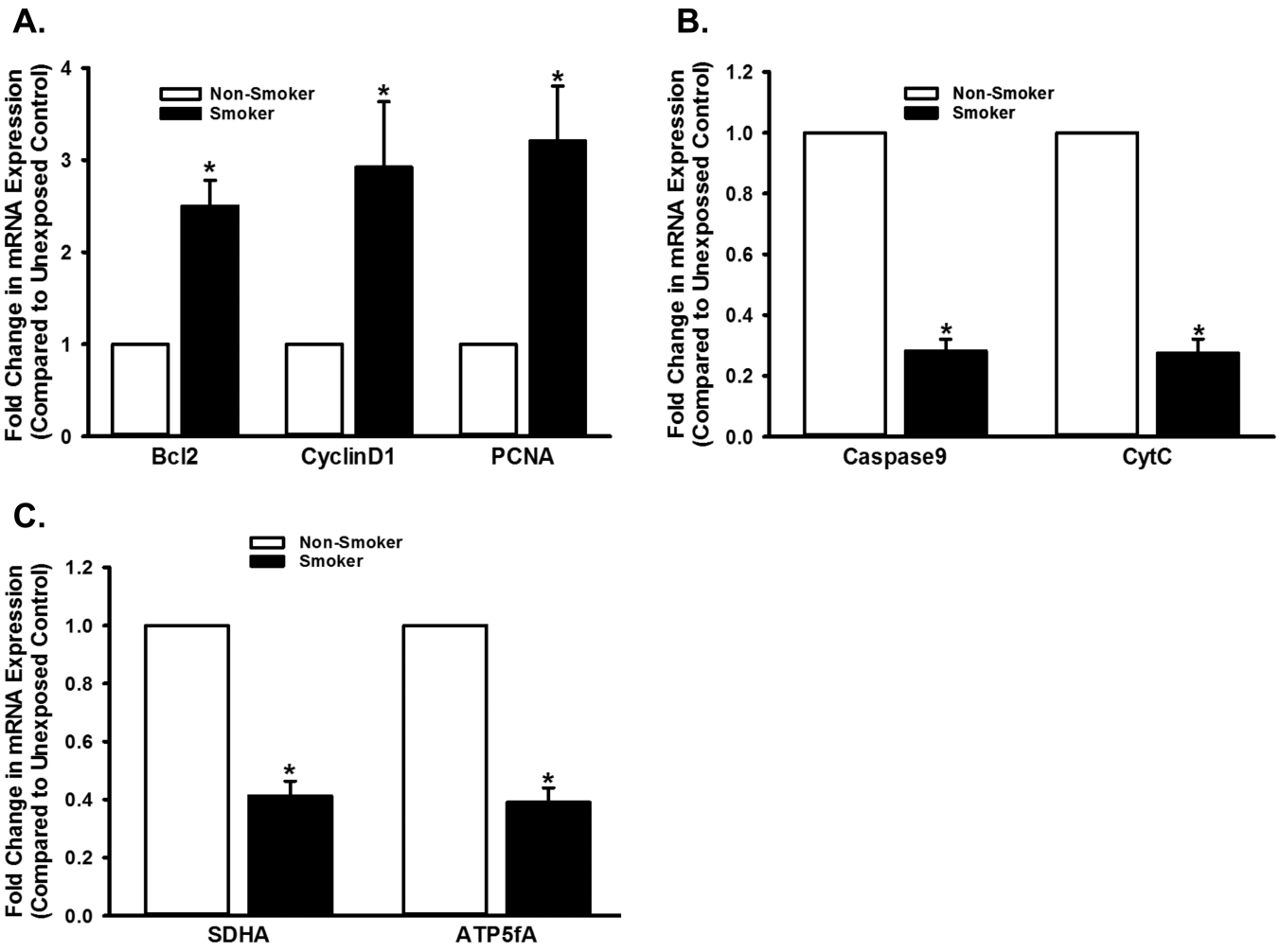

Figure 9. Chronic exposure to CS modulates multiple aspects of mitochondrial function in the airway

ASM layer was obtained from unexposed and CS-exposed mice (see Methods for details), using LCM. Messages corresponding to proteins involved in cell proliferation, apoptosis, and ETC were analyzed and quantified by real-time PCR. Quantifiable changes in mRNA expression were observed: CS upregulates proliferation **(A)**, marked by an increase in the expression of Bcl2, CyclinD1 and PCNA. Expression of apoptosis markers Caspase9 and CytC **(B)**, and ETC markers SDHA and ATP5A **(D)** are decreased in CS exposed airways, compared to unexposed controls. Ribosomal protein S16 was used as reference, and unexposed control was used as the calibrator. (N=16; * indicates significant difference from unexposed control; $P<0.05$).

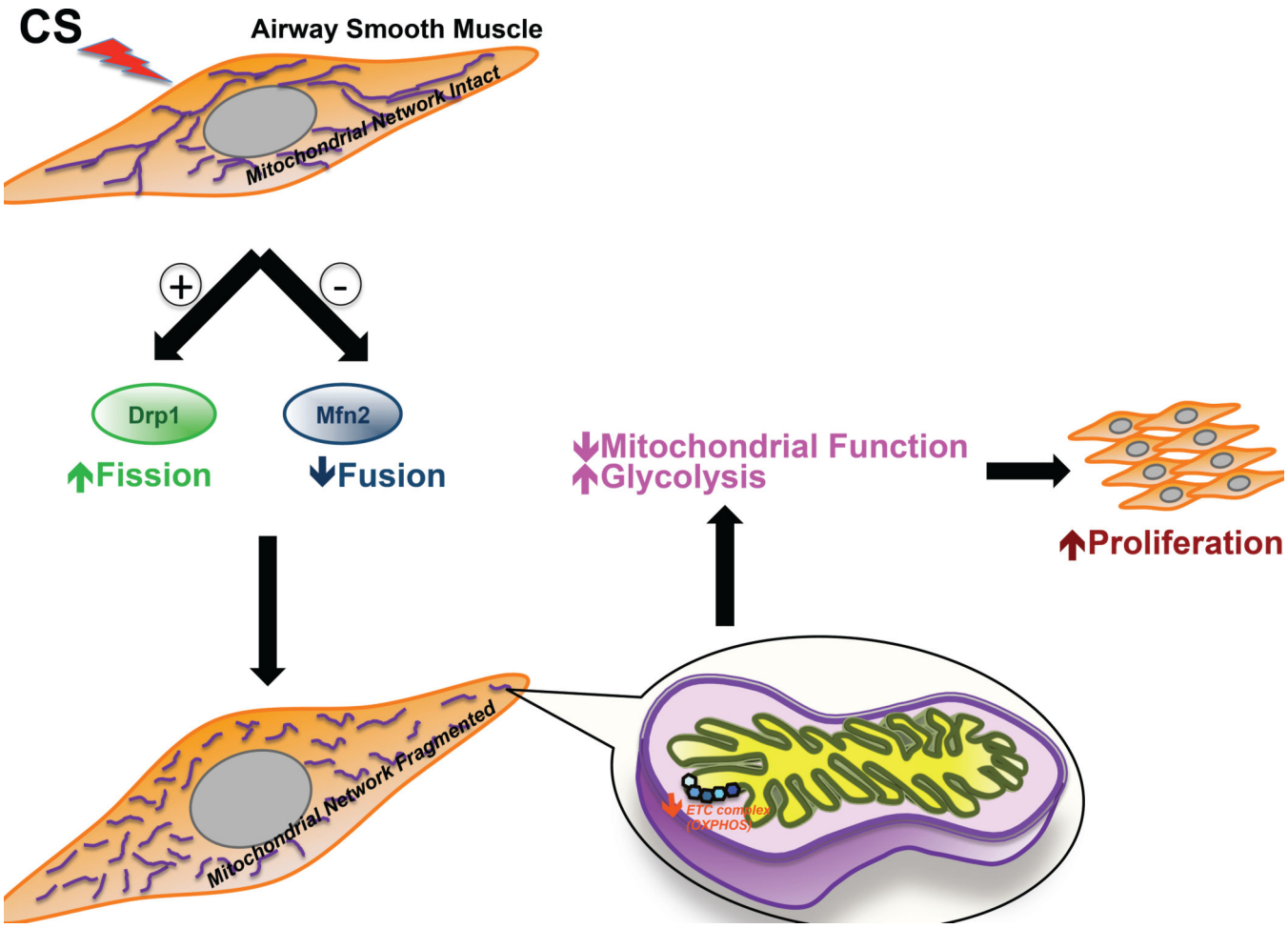

Figure 10. CS-induced changes in mitochondrial morphology lead to mitochondrial dysfunction and ASM proliferation

Model depicting the effects of CS exposure on ASM. CS disrupts mitochondrial networking in the ASM by decreasing the expression of the fusion protein Mfn2 and increasing the expression of the fission protein Drp1. In consequence, the bioenergetic function of mitochondria becomes defective, making ATP production more dependent on glycolysis than on oxidative phosphorylation. This switch in metabolic pathway preference (along with other possible mechanisms such as increased ROS production, and increased autophagy/mitophagy) promotes cell proliferation contributing to airway remodeling.

Table 1
Oligonucleotide primers for PCR of LCM-dissected ASM tissue

Forward and reverse primers specific for mouse amplicons targeted in the current study were obtained from Integrated DNA Technologies. Primers were used at a final concentration of 500nM in the quantitative real-time PCR reactions.

Primer ID	Sequence
mATP5A	*5′ATGCAATCGACATGGAGAAGGCACAG3′/5′TGCGACGCATCATGTTCTGTACAGAG3′*
mBcl2	*5′GAGAACAGGGTATGATAACCGGGAGA3′/5′TTGCTCTCAGGCTGGAAGGAGAAGAT3′*
mCaspase9	*5′CCTTCCTCTCTTCATCTCCTGCTTAG3′/5′TCTGCTCCTTTGCTGTGAGTCCCATT3′*
mCyclinD1	*5′AGAACCTGTTGACCATCGAGGA3′/5′GGCTGAGGATTCTGGGTAGAAGT3′*
mCytC	*5′TTTGTTCAGAAGTGTGCCCAGTGCCA3′/5′AATACTCCATCAGGGTATCCTCTCCC3′*
mPCNA	*5′GGCTCTCAAAGACCTCATCAATGAGG3′/5′CCCGACTTCTATTACGTCTGTGGA3′*
mS16	*5′TGCAGGTCTTCGGACGCAAGAAAA3′/5′CGAATATCCACACCAGCAAATCGC3′*
mSDHA	*5′TGCGGCTTTCACTTCTCTGTTGGTGA3′/5′GCATGCAGTATTAAACCCTGCCTCAG3′*

Table 2
Oligonucleotide primers for Q-PCR on human ASM

Forward and reverse primers specific for human amplicons targeted in the current study were obtained from Integrated DNA Technologies. Primers were used at a final concentration of 500nM in the quantitative real-time PCR reactions.

Primer ID	Sequence
hATP5A	*5′TCTTCAGAGGCTCTTCAGGTTCTCCT3′/5′ATCAACAGGTCCTCCAGATGTCTGTC3′*
hBcl2	*5′CCTGTGGATGACTGAGTACCTGAA3′/5′AACTGAGCAGAGTCTTCAGAGACAGC3′*
hCaspase9	*5′AGGCAGCTGATCATAGATCTGGAGAC3′/5′ACCACTGGGGTAAGGTTTTCTAGGGT3′*
hCyclinD1	*5′GAGAAGCTGTGCATCTACACCGACAA3′/5′TGCGGATGATCTGTTTGTTCTCCTCC3′*
hCytC	*5′TGGGTGATGTTGAGAAAGGCAAG3′/5′CTTATTGGCGGCTGTGTAAGAG3′*
hPCNA	*5′ATCCTCAAGAAGGTGTTGGAGGCACT3′/5′TTTGGACATACTGGTGAGGTTCACGC3′*
hS16	*5′CAATGGTCTCATCAAGGTGAACGG3′/5′CTGACGGATAGCATAAATCTGGGC3′*
hSDHA	*5′AACAGTGTTGCAAACAGGAACCCGAG3′/5′GTATTAAACCCTGCCTCAGAAAGGCC3′*

Table 3

Summary of mRNA expression analysis of mitochondrial function markers

Total RNA, isolated from ASM cells (transfected with Drp1siRNA or Mfn2siRNA, and exposed to 1% CSE), was reverse transcribed and resultant cDNA used as a template in real-time PCR. Expression of multiple messages, corresponding to proteins involved in various functions of the mitochondria, namely proliferation, apoptosis, and energy metabolism, was analyzed. Results from experiments on four different ASM populations are summarized. Values are presented: means ± SE.

TF	Vehicle	Vehicle	Non-specific RNA	Non-specific RNA	Drp1 siRNA	Drp1 siRNA	Mfn2 siRNA	Mfn2 siRNA
1% CSE	−	+	−	+	−	+	−	+
CyclinD1	1 ± 0	2.805 ± 0.737	1.029 ± 0.165	3.128 ± 0.57	0.4204 ± 0.076	1.114 ± 0.085	2.882 ± 0.313	6.671 ± 0.901
Bcl2	1 ± 0	2.677 ± 0.345	1.135 ± 0.214	2.541 ± 0.328	0.456 ± 0.166	1.786 ± 0.216	2.353 ± 0.167	3.757 ± 0.536
CytC	1 ± 0	0.372 ± 0.049	1.0177 ± 0.138	0.376 ± 0.053	2.106 ± 0.238	1.354 ± 0.093	0.408 ± 0.055	0.252 ± 0.043
ATP5A	1 ± 0	0.283 ± 0.040	1.074 ± 0.127	0.323 ± 0.061	0.359 ± 0.032	0.177 ± 0.0276	2.418 ± 0.203	1.346 ± 0.105

Table 4

Summary of protein expression analysis of mitochondrial function markers

Total protein, isolated from ASM cells (transfected with Drp1- or Mfn2 siRNA, and exposed to 1% CSE), was subjected to immunoblotting. Expression of multiple proteins, involved in the various functions of the mitochondria, namely proliferation, apoptosis, and energy metabolism, was analyzed. Specific bands were quantified by densitometry. Results from experiments on four different ASM populations are summarized. Values are presented: means ± SE.

TF	Vehicle	Vehicle	Non-specific RNA	Non-specific RNA	Drp1 siRNA	Drp1 siRNA	Mfn2 siRNA	Mfn2 siRNA
1% CSE	−	+	−	+	−	+	−	+
CyclinD1	1 ± 0	1.707 ± 0.108	1.000 ± 0.043	1.707 ± 0.165	0.427 ± 0.054	0.759 ± 0.127	1.653 ± 0.050	2.223 ± 0.13937
Bcl2	1 ± 0	1.695 ± 0.112	1.011 ± 0.029	1.709 ± 0.122	0.462 ± 0.058	0.786 ± 0.108	1.697 ± 0.098	2.3487 ± 0.234
Caspase3	1 ± 0	0.713 ± 0.008	1 ± 0	0.728 ± 0.012	1.386 ± 0.044	0.92 ± 0.035	0.7 ± 0.015	0.492 ± 0.013
CytC	1 ± 0	0.586 ± 0.025	0.987 ± 0.0187	0.577 ± 0.022	1.332 ± 0.0231	0.935 ± 0.0224	0.587 ± 0.03	0.415 ± 0.018
ATP5A	1 ± 0	0.626 ± 0.049	1.023 ± 0.025	0.61 ± 0.048	0.643 ± 0.055	0.453 ± 0.0532	1.414 ± 0.046	1.013 ± 0.054
LDHA	1 ± 0	1.346 ± 0.026	0.969 ± 0.014	1.337 ± 0.022	0.535 ± 0.01	0.727 ± 0.012	1.505 ± 0.013	1.794 ± 0.039